

# The impact of weather and atmospheric circulation on O<sub>3</sub> and PM<sub>10</sub> levels at a rural mid-latitude site

M. Demuzere<sup>1,2</sup>, R. M. Trigo<sup>2</sup>, J. Vila-Guerau de Arellano<sup>3</sup>, and N. P. M. van Lipzig<sup>1</sup>

<sup>1</sup>Earth and environmental Sciences, Celestijnenlaan 200E, 3001 Heverlee (Leuven), Katholieke Universiteit Leuven, Belgium

<sup>2</sup>Centro de Geofísica da Universidade de Lisboa (CGUL), IDL, University of Lisbon, Fac. Ciências, Campo Grande, Ed. C8, Piso 6, 1749-016 Lisbon, Portugal

<sup>3</sup>Meteorology and Air Quality Section, Wageningen University, Droevendaalsesteeg 4, P.O. Box 47, 6700 AA Wageningen, The Netherlands

Received: 22 August 2008 – Published in Atmos. Chem. Phys. Discuss.: 16 December 2008

Revised: 20 March 2009 – Accepted: 10 April 2009 – Published: 23 April 2009

**Abstract.** In spite of the strict EU regulations, concentrations of surface ozone and PM<sub>10</sub> often exceed the pollution standards for the Netherlands and Europe. Their concentrations are controlled by (precursor) emissions, social and economic developments and a complex combination of meteorological actors. This study tackles the latter, and provides insight in the meteorological processes that play a role in O<sub>3</sub> and PM<sub>10</sub> levels in rural mid-latitudes sites in the Netherlands. The relations between meteorological actors and air quality are studied on a local scale based on observations from four rural sites and are determined by a comprehensive correlation analysis and a multiple regression (MLR) analysis in 2 modes, with and without air quality variables as predictors. Furthermore, the objective Lamb Weather Type approach is used to assess the influence of the large-scale circulation on air quality. Keeping in mind its future use in downscaling future climate scenarios for air quality purposes, special emphasis is given to an appropriate selection of the regressor variables readily available from operational meteorological forecasts or AOGCMs (Atmosphere-Ocean coupled General Circulation Models). The regression models perform satisfactory, especially for O<sub>3</sub>, with an  $R^2$  of 57.0% and 25.0% for PM<sub>10</sub>. Including previous day air quality information increases significantly the models performance by 15% (O<sub>3</sub>) and 18% (PM<sub>10</sub>). The Lamb weather types show a seasonal distinct pattern for high (low) episodes of average O<sub>3</sub> and PM<sub>10</sub> concentrations, and these are clear related with the meteorology-air quality correlation analysis. Although using

a circulation type approach can provide important additional physical relations forward, our analysis reveals the circulation method is limited in terms of short-term air quality forecast for both O<sub>3</sub> and PM<sub>10</sub> ( $R^2$  between 0.12 and 23%). In summary, it is concluded that the use of a regression model is more promising for short-term downscaling from climate scenarios than the use of a weather type classification approach.

## 1 Introduction

Ground-level ozone (O<sub>3</sub>) and particulate air pollution (PM<sub>10</sub>) have been identified as two of the most important air pollutants for Europe in general (Jol and Kielland, 1997; Brunekreef and Holgate, 2002) and over the Benelux region in particular (Tulet et al., 2000). Since their adverse health effects have been observed for decades, the supervising European institutions have produced appropriate legislation and several emission reduction measures have been taken to reduce ambient air pollution (European Community, 1999; WHO, 2000, 2005). Nevertheless, levels of O<sub>3</sub> and PM<sub>10</sub> continue to exceed frequently the target values and the long-term objectives established in EU legislation. Moreover, international literature shows that air pollution continues to be detrimental to human health despite these emission standards (van der Wal and Janssens, 2000; Medina et al., 2004; Schlink et al., 2006).

In recent decades, typical causes of high ozone and PM<sub>10</sub> pollution received ample treatment in the scientific literature. Relatively high levels of these pollutants are usually associated to the close proximity of high precursor emissions and



Correspondence to: M. Demuzere  
(matthias.demuzere@ees.kuleuven.be)

as a result of industrial and societal developments. Moreover, ambient air pollution is also strongly influenced by meteorological factors, due to a complex combination of processes and influences, namely; emission, transport, chemical transformations, and removal via wet and dry processes (Seinfeld and Pandis, 1998). Thus, weather/climate elements play a significant role in all these processes' components. On a local scale, emission (e.g., biogenic or dust emissions) may depend on climate variables such as temperature and surface wetness; (photo) chemical processes depend on temperature, humidity, solar radiation fluxes and cloudiness; the precipitation process influences wet removal. From a regional point of view, short and long-term transport depends on the magnitude of surface turbulence and on the atmospheric circulation (at the synoptic scale). This means that the distribution of pollutants is not only dependent on the spread of its emissions, but is also affected by various weather/climatic drivers (Giorgi and Meleux, 2007).

Over the last few decades, the effects of chemical tracers on climate change have been investigated extensively (Intergovernmental Panel on Climate Change, 2007). Conversely, comparatively less attention has been devoted to the issue of climate-change effects on air quality (Andersson and Langner, 2007a; Jacobson, 2008). However, we believe that, in order to understand the full range of atmospheric processes that govern the evolution of air quality under a changing climate, one has to understand and quantify the processes that impact on the atmospheric pollutants on a present time scale. Air quality is affected by both local (in situ) and regional scale processes on a few tens and hundreds kilometers. As current AOGCMs (Atmospheric-Ocean Coupled Global Climate Models) are only capable of resolving phenomena at the resolution of a few hundreds of kilometers, the climate change-air quality interactions are hampered. Furthermore, many chemical atmospheric elements, and particularly those with adverse impacts on human health, such as tropospheric O<sub>3</sub> and PM<sub>10</sub>, have a lifetime of the order of some hours to days (Seinfeld and Pandis, 1998). As a result, their distribution is highly variable in space and time and is often tied to the distribution of sources (Giorgi and Meleux, 2007).

The main aim of this paper is to study the above-mentioned weather climatology-air quality relation at both the regional and local spatial scales. On the one hand, weather-air quality interactions on the local-scale are quantified based on techniques often used in short-term air quality forecasts. Here, the selection of an appropriate method depends on its simplicity, practical feasibility, sufficient accuracy and should be computationally inexpensive, so that it can easily be applied to output of different climate models (Semazzi, 2003). The latter rules out the use of a complex climate-air quality modelling system (in off-or online mode), a field of research that has been reviewed comprehensively recently by Giorgi and Meleux (2007).

Many empirical prediction models have been developed to investigate the relationships between meteorological and air

quality data. Numerous reports describe model results on different air quality variables and different locations from multiple linear regression (MLR) analysis (Hubbard and Cobourn, 1998; Barrero et al., 2006; Stadlober et al., 2008), nonlinear multiple regressions (Cobourn, 2007), artificial neural networks (ANN) (Gardner and Dorling, 1998; Nunnari et al., 1998; Reich et al., 1999; Benvenuto and Marani, 2000; Perez et al., 2000; Perez, 2001; Kukkonen et al., 2003; Hooyberghs et al., 2005; Papanastasiou et al., 2007), generalized additive models and fuzzy-logic-based models (Cobourn et al., 2000). Other authors compared several methods on a single dataset (from the same measurement site) or combined various approaches in order to improve the specific air pollutant forecast (Agirre-Basurko et al., 2006; Goyal et al., 2006; Al-Alawi et al., 2008). Comrie (1997) compared the potential of traditional regression and neural networks to forecast ozone pollution under different climate and ozone regimes. Model comparison statistics indicate that neural network techniques are only slightly better than regression models for daily ozone prediction. Cobourn et al. (2000) compared nonlinear regression and neural network models for ground-level ozone forecasting in Louisville (USA). They conclude that both models performed essentially the same, as measured by various errors statistics. In contrast, Gardner and Dorling (2000), concluded that significant increase in performance is possible when using MLP models, whereas the use of regression models are more readily interpretable in terms of the physical mechanisms between meteorological and air quality variables.

Taking into account results obtained in previous research showing a similar performance between linear regression and neural network techniques, we decided to employ here a stepwise multiple linear regression model which guarantees, simultaneously, robustness and simplicity. Practical feasibility is obtained by including these parameters that are provided/forecasted individually by AOGCMs/operational models. On the other hand, the discriminative power of a circulation classification method is tested as an air quality assessment tool, keeping in mind its potential future use in downscaling future climate scenarios for air quality purposes (Huth et al., 2008). Prior to the selection of variables for the model, a comprehensive correlation study is conducted between the meteorological and air quality variables. Afterwards, levels of O<sub>3</sub> and PM<sub>10</sub> are reconstructed using a stepwise multiple linear regression technique and a circulation pattern approach. Finally, both methodologies results are objectively compared, with the aim of stressing their corresponding strengths and weaknesses for long-term air quality assessment studies.

To the best of our knowledge, this approach has never before been conducted for the Benelux area. In fact, this integrated approach connects both atmospheric chemistry on the local scale using observations from rural sites in the Netherlands and synoptic climatology based on ECMWF (European Centre for Medium-range Weather Forecasting) operational

**Table 1.** Characteristics of the meteorological and air quality measurement sites in the Netherlands for the period 2001–2006.

Code	Location	Latitude	Longitude	Height (m)	Start measurements	End measurements	Available variables (see Table 1 for description)
<i>Meteorological stations (KNMI)*</i>							
375	Volkel	52.07° N	6.65° E	20.1	01/03/1951	Present	DD, FF, Tmean, Tmin, Tmax, Rain, P0, RH
340	Woensdrecht	51.45° N	4.35° E	14.9	02/05/1995	Present	DD, FF, Tmean, Tmin, Tmax, P0, RH
283	Hupsel	51.65° N	5.7° E	29	01/01/1990	Present	DD, FF, Tmean, Tmin, Tmax, RH
348	Cabauw	51.97° N	4.296° E	−0.7	01/01/1997	Present	DD, FF, Tmean, Tmin, Tmax, SWD, RH, P0, CC, Td, Rain
<i>Air quality stations (RIVM -AIRBASE)</i>							
232	Volkel	52.07° N	6.65° E	20.1	Depends on the variable		O <sub>3</sub> , NO, NO <sub>2</sub> , SO <sub>2</sub>
235	Woensdrecht	51.45° N	4.35° E	14.9	Depends on the variable		O <sub>3</sub> , NO, NO <sub>2</sub> , SO <sub>2</sub> , PM <sub>10</sub>
722	Hupsel	51.65° N	5.7° E	29	Depends on the variable		O <sub>3</sub> , NO, NO <sub>2</sub>
620	Cabauw**	51.97° N	4.296° E	−0.7	Depends on the variable		O <sub>3</sub> , NO, NO <sub>2</sub> , SO <sub>2</sub>
633	Zegveld**	52.139° N	4.838° E	3	Depends on the variable		PM <sub>10</sub>

\* A more detailed description of these measurement stations is available at: <http://www.knmi.nl/klimatologie/daggegevens/download.html>

\*\* Cabauw and Zegveld are neighbouring air quality measurement stations (<20 km) and are hereafter referred to as Cabauw (620).

analysis data. Although the different aspects of the methodology are widely used in their specific field of application, they are seldom compared against each other. Many authors solely used the first step in forecasting future levels of air quality variables (e.g. Oanh et al., 2005; Wise and Comrie, 2005), while many studies investigated air quality in relation to the latter (Comrie, 1992; Davies et al., 1992a, b; Cannon et al., 2002; Kassomenos et al., 2003; Bridgeman and O'Connor, 2007). An objective combination of both methodologies results in a further insight in weather-air quality related issues, and presents their corresponding (dis)advantages for long-term air quality assessment studies.

## 2 Data

In order to get insight in the weather-air quality interactions on the local and regional scale, different sets of meteorological and air quality data are used and described in the following sections.

### 2.1 ECMWF operational data

We have extracted large-scale operational data from the ECMWF (European Centre for Medium Weather Forecast) on a 2.5° × 2.5° grid for the larger European Atlantic Region (20° W–35° E, 75° N–35° N). This dataset is used to determine prevailing circulation patterns at the regional scale. The data covers the 2001–2004 period, identical to the period selected to construct the linear model from the measurements described in Sect. 2.2. For the circulation pattern approach, 12 h UTC mean sea level pressure (MSLP) is used, while mean temperature (K) and relative humidity (%) are daily averaged from the four provided time steps for the period

2001–2004. In order to compute the long-term climatological normal, we have extracted 12h UTC MSLP and daily mean temperature and relative humidity for the period 1971–2000.

### 2.2 Local meteorological measurements

Previous efforts to relate air quality variable concentration data to surface meteorological variables have shown that temperature (Smith et al., 2000), wind speed, relative humidity, and cloud cover are relevant variables (NRC, 1991). Other meteorological-air quality studies have found wind direction, dew point temperature, sea level pressure and precipitation useful in the modelling and forecasting of air quality variables (Gardner and Dorling, 1999; Delcloo and De Backer, 2005; Hooyberghs et al., 2005; Grivas and Chaloulakou, 2006; Andersson et al., 2007a, b; Papanastasiou et al., 2007). Furthermore, Comrie (1997) states that the use of several types of models for ozone prediction can be particularly sensitive to different weather-ozone regimes and urban measurement locations. In order to by-pass this complexity, this study solely uses measured high-temporal resolution data from rural sites. This is done in order to get insight into the meteorological – air quality interactions with a limited interference from local emission sources, implying a limitation of this approach to sites where the variability of emissions is of minor importance. In this respect, we have only considered measurements from rural observation sites, with a daily (or higher) temporal resolution meteorological measurements for the period 2001–2006 and with the availability of air quality measurements (see Sect. 2.3). This results in a selection of 4 rural stations located in central and southern sections of the Netherlands (Table 1 and Fig. 1).

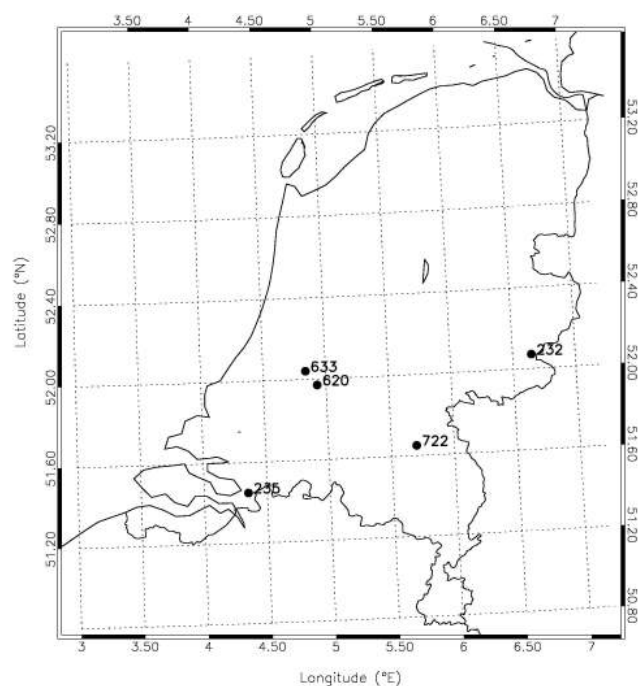


**Fig. 1.** Location of the rural meteorological and air quality measurement sites in the Netherlands.

For all stations, wind speed (FF) and direction (DD), daily mean (Tmean), minimum (Tmin) and maximum (Tmax) temperature and relative humidity (RH) are available. For Cabauw and Volkel, additional information is available on daily mean precipitation (Rain). Furthermore, all stations (except Hupsel) measure sea level pressure (P0). Cabauw has additional information on shortwave downward radiation (SWD) and cloud cover (CC). As Cabauw has no direct measurements of relative humidity, shown by Barrero et al. (2006) to correlate significantly ( $p < 0.01$ ) with suspended particles, NO<sub>2</sub>, SO<sub>2</sub> and O<sub>3</sub>, the relation between 2 m air and 2 m dew point temperature is used to derive the relative humidity. A quality control was performed at the KNMI (Royal Dutch Meteorological Institute) whereby quality numbers for each measured parameter are defined in the same way as in the former continuous Cabauw programme (Beljaars and Bosveld, 1997). After removal of spurious data, the measurements are averaged to daily values, in order to be able to make a connection with coarsely spatial and temporal gridded data from ECMWF operational analysis or AOGCMs. As for the air quality variables (see Sect. 2.3), the first 4 years are used to build the regression model, while the period 2005–2006 is used to validate the model.

### 2.3 Air quality data

In addition to the meteorological variables, NO, NO<sub>2</sub> and SO<sub>2</sub> concentrations are added as independent variables explaining the variation of O<sub>3</sub> and PM<sub>10</sub>. The air qual-

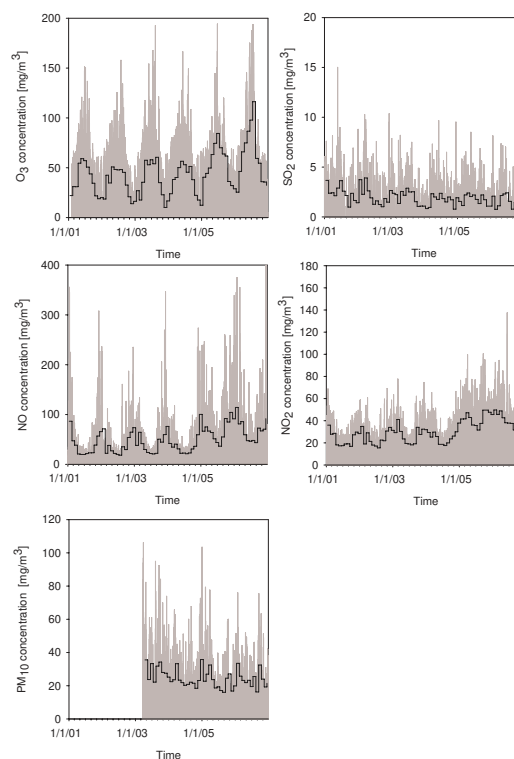


**Fig. 2.** Time series of daily (grey bars) and monthly mean (black line) values for surface O<sub>3</sub>, NO, NO<sub>2</sub>, SO<sub>2</sub> and PM<sub>10</sub> measured at Cabauw/Zegveld between the period 2001–2006 (March 2003–2006 for PM<sub>10</sub>).

ity data was obtained from the AIRBASE database (<http://air-climate.eionet.europa.eu/databases/EuroAirnet/>). Hourly measurements of O<sub>3</sub>, NO, NO<sub>2</sub> and SO<sub>2</sub> are selected from the rural stations where available, for the period 2001–2006. Again, these locations are chosen with the expectation that, by selecting a rural background station, non-local correlations would be more clearly revealed and that the confounding effect of local urban vehicular NO<sub>x</sub> emissions will be limited (Gardner and Dorling, 2000). Taking into account the use of meteorological variables on a daily scale, a representative daily value is considered for each pollutant. For SO<sub>2</sub> and PM<sub>10</sub> daily means are considered, while for O<sub>3</sub> the daily 8-hourly maximum mean and for NO and NO<sub>2</sub> the daily maximum value is used (European Community, 1999).

Monthly and annual cycles are clearly revealed for O<sub>3</sub>, NO and NO<sub>2</sub> (Fig. 2). The yearly cycles of O<sub>3</sub> reveal the highest peak concentrations in summer, whereas for NO and NO<sub>2</sub>, the annual cycle is characterized by a summer minimum and a maximum in winter. This can be understood from the mutual relation between O<sub>3</sub>, NO and NO<sub>2</sub> in which the oxides of nitrogen (next to CO and volatile organic compounds (VOC) react with the hydroxyl radical OH) as precursors in

the nonlinear chemical process forming O<sub>3</sub> (NRC, 1991; Sillman, 1999; Satsangi et al., 2004; Lasry et al., 2005). In this respect, scientists have attempted to characterize local regions as “NO<sub>x</sub>-limited” and “VOC-limited” with respect to the reduction of photo-oxidant formation. The regime in a particular region will depend principally on the concentration of NO<sub>x</sub> and the VOC/NO<sub>x</sub> ratio. Thereby, urban areas are often denoted as “VOC-limited” (lower VOC concentrations), whereas rural and suburban areas are denoted as “NO<sub>x</sub>-limited” (lower NO<sub>x</sub> concentrations) (Reis et al., 2000). Here, NO<sub>x</sub> acts as a catalyst and produces O<sub>3</sub> until its removal as NO<sub>3</sub> by deposition processes or its conversion into other forms of nitrogen. More detailed information on the photochemical reactions forming ozone under varying NO<sub>x</sub> and volatile organic compounds emissions can be found in Sillman and He (2002). For SO<sub>2</sub> and PM<sub>10</sub>, concentration levels are rather constant throughout the year. The highest monthly SO<sub>2</sub> concentrations are reached in January and June, while the maximum daily concentration is reached in March. Additionally, differences among the seasons can be considered relatively small (<1 standard deviation).

In order to know whether different rural sites in the Netherlands have similar characteristics in terms of O<sub>3</sub> and PM<sub>10</sub> concentrations, the annual cycle for all selected sites is depicted in Fig. 3. Concerning O<sub>3</sub> it is found that the highest median concentrations are observed in spring months (MAM) for all stations, whereas peak concentrations occur in summer (JJA). This refers to the presence of a spring and summertime maximum often seen in midlatitudes (Delcloc and De Backer, 2008). As it is also shown by Fig. 2, the lowest daily medians of surface ozone concentrations are found in November, December and January. For PM<sub>10</sub>, maximum daily mean concentrations are found in June and December, while in Cabauw and Woensdrecht a less distinct peak can be observed in February and March. Furthermore, it is clear that for both O<sub>3</sub> and PM<sub>10</sub>, all sites are characterized by similar annual cycles in terms of their median concentrations. Furthermore, the Directive 1999/30/EC and following up Directive 2008/50/EC of the European Parliament (EU, 1999, 2008) impose a threshold concentration of 120 μg/m<sup>3</sup> and 50 μg/m<sup>3</sup> for a maximum eight-hourly mean O<sub>3</sub> and daily mean PM<sub>10</sub> concentration respectively for Europe. The number of days exceeding these thresholds for the different rural sites range between 3–4.5% yr<sup>-1</sup> for O<sub>3</sub> and 6.2–8% yr<sup>-1</sup> for PM<sub>10</sub>. This shows that there are only minor differences in O<sub>3</sub> and PM<sub>10</sub> concentrations for different rural measurement sites in the Netherlands, as was also suggested by Flemming et al. (2005) for other rural areas.

### 3 Methods

It is now widely accepted that there are two main approaches in synoptic climatology to investigate the links between local-scale environmental features and large-scale circula-

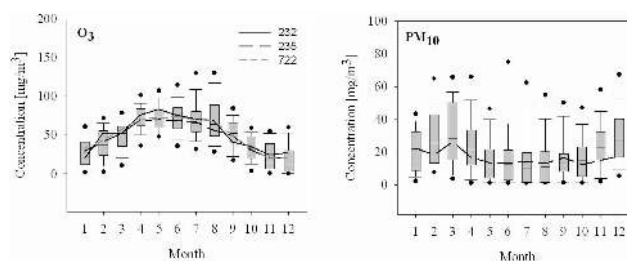


**Fig. 3.** Monthly distribution of O<sub>3</sub> and PM<sub>10</sub> concentrations for Cabauw/Zegveld (as Box-Whiskers), Volkel (232), Woensdrecht (235) and Hupsel (722). The boxes present the median, the first and third quartiles, while the whiskers and dots present the minimum and maximum value and possible outliers respectively.

tion patterns (Yarnal, 1993): the environment-to-circulation approach and the circulation-to-environment approach. The former structures the circulation data based on criteria defined by the environmental variable and lacks any capability in a predictive mode, but can be of use in a descriptive way to get more insight in those patterns that are regulating the magnitude of surface environmental variables. Conversely, the latter classifies the circulation data based on standard pressure fields (e.g. SLP or 500 hPa geopotential height), prior to seeking links with the local-scale environment. In this study, we adopt the latter, which has the capability to calculate expected air quality conditions related to each circulation pattern, and to compare this forecast with the observed air quality values to evaluate the strength of the circulation-to-environmental approach (Cannon et al., 2002).

#### 3.1 Stepwise regression analysis

Our goal is to model the maximum 8-hourly mean O<sub>3</sub> and mean daily PM<sub>10</sub> levels by a linear model that will form the basis for our understanding and reconstruction of the air quality variables based on local-scale meteorological and air quality observations. For this purpose, we use a robust approach based on stepwise multiple linear regression models for both the dependent variables O<sub>3</sub> and PM<sub>10</sub>.

Prior to the regression analysis we assess the linear nature of the relationship between the dependent and independent datasets. In case these relations are non-linear, an appropriate variable transformation is applied in order to assure linearity. Secondly, the data is checked for the existence of multicollinearity. If the tolerance (a measure for the strength of a linear relationship among the independent variables) between two variables is below a threshold value of 0.1 (Norusis, 2002), then these variables are highly related and their simultaneous use can be misleading and interfere with a correct interpretation of the regression results. In such a situation, the variables that suffer from multicollinearity should be identified and some of them removed from the rest of the analysis. Only then we apply the multiple linear regression with a stepwise method for variable selection to reconstruct

time series for O<sub>3</sub> and PM<sub>10</sub> with F probability <0.05 to enter and F probability <0.10 to exit. The model was developed with the data subset covering the whole period, from 1 January 2001 to 31 December 2004. Missing data was treated following a listwise deletion (Norusis, 2002), which means that for PM<sub>10</sub>, only the period from 20th of March 2003 until 31st of December 2004 is considered.

### 3.2 Circulation-to-environmental approach

As our aim is to test the circulation patterns as a future air quality assessment tool, the circulation-to-environmental approach will be followed using the automated Lamb Weather Types (hereafter called WTs) adapted from Jenkinson and Collison (1977) and Jones et al. (1993) to the Low Countries. The rationale for using this approach is that the identification of a clear link between circulation patterns and air quality variables could be used as a downscaling tool for air quality assessment, using operational analysis or AOGCM data as input.

The WTs are developed using ECMWF MSLP data and for a given day they describe the location of the high- and low-pressure centers that determine the direction of the geostrophic flow. A grid with 16 points is assigned over the larger Western and Central Europe, with a central point over the Benelux, in 52.5° N and 5° E (Fig. 4). We computed a set of simple atmospheric circulation indices using mean sea level pressure (MSLP) at 12UTC in these 16 grid points, namely the direction and vorticity of geostrophic flow: southerly flow (SF), westerly flow (WF), total flow (F), southerly shear vorticity (ZS), westerly shear vorticity (ZW) and total shear vorticity (Z). A small number of empirical rules devised previously (Jones et al., 1993; Trigo and Da-Camara, 2000) are then used to classify each day as one of the 27 circulation types recently developed in Demuzere et al. (2008).

### 3.3 Model evaluation measures

Statistical model performances are evaluated using appropriate scalar measures and skill scores (Wilks, 1995), namely: the Pearson correlation coefficient (R), mean square error (MSE), root mean square error (RMSE) and explained variance in% ( $R^2$ ). According to Murphy (1988), the skill of any given model is a measure of the relative accuracy of a model with respect to a standard reference model. Hence, the skill of any model should be interpreted as the percentage improvement over a reference or benchmark model (Wilks, 1995). The two most commonly applied reference models used in atmospheric sciences are climatology and persistence. Therefore, two skill scores based on the MSE will be used in this paper with the climatological mean ( $MSE_{\text{clim}}$ ) and the persistence ( $MSE_{\text{pers}}$ ) as a reference:

$$SS_c(\text{MSE}) = \frac{\text{MSE} - \text{MSE}_{\text{clim}}}{0 - \text{MSE}_{\text{clim}}} \times 100\%$$

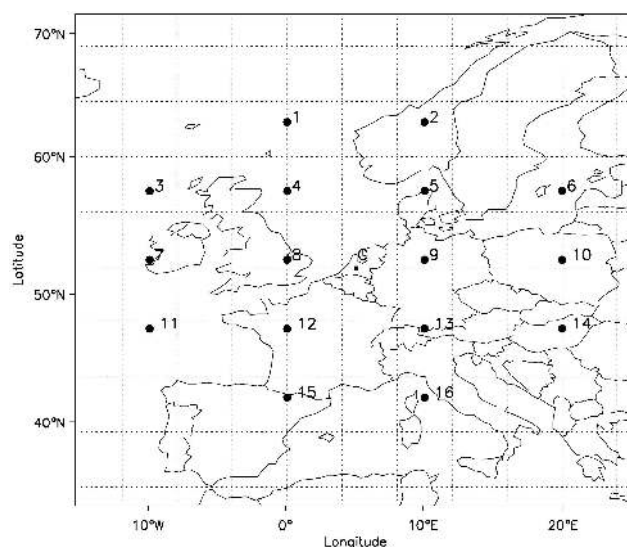


**Fig. 4.** Location of the 5°×10° MSLP grid used, with 16 point centered over the Benelux. “C” denotes the location of the Cabauw measurement station and the grid center.

$$SS_p(\text{MSE}) = \frac{\text{MSE} - \text{MSE}_{\text{pers}}}{0 - \text{MSE}_{\text{pers}}} \times 100\%$$

with the “0” corresponding to the accuracy level that would be achieved by a perfect model.

Furthermore, the Kruskal-Wallis one-way analysis of variance is used as a non-parametric method to test the difference of O<sub>3</sub> and PM<sub>10</sub> population medians among the weather type groups (Kruskal and Wallis, 1952). A 1% significance level is used and hereafter denoted as  $\alpha_{KW}$  in Sect. 4.3.

## 4 Results and discussion

### 4.1 Diurnal, seasonal and annual cycles

Prior to the selection of the weather and air quality variables for the regression analysis, their mutual relations are investigated as a function of time. Therefore, Pearson correlation coefficients are calculated between each of the selected air quality and meteorological variables for each month separately in (Figs. 5 and 6). We have used anomalies of each variable in order to remove the annual cycle. Furthermore, we have taken into account autocorrelation effects when computing the Pearson correlation values. Hence, the sample size  $n$  is replaced by an effective (smaller) sample size  $n_{\text{eff}}$  that returns the Pearson correlation coefficient with its respective “adjusted” level of significance (Santer et al., 2000). Previous works have stressed the existence of temporal lags on the relations between air quality and meteorological variables (Kalkstein and Corrigan, 1986; Styer et al., 1995; Ziomas et al., 1995; Cheng and Lam, 2000). In order



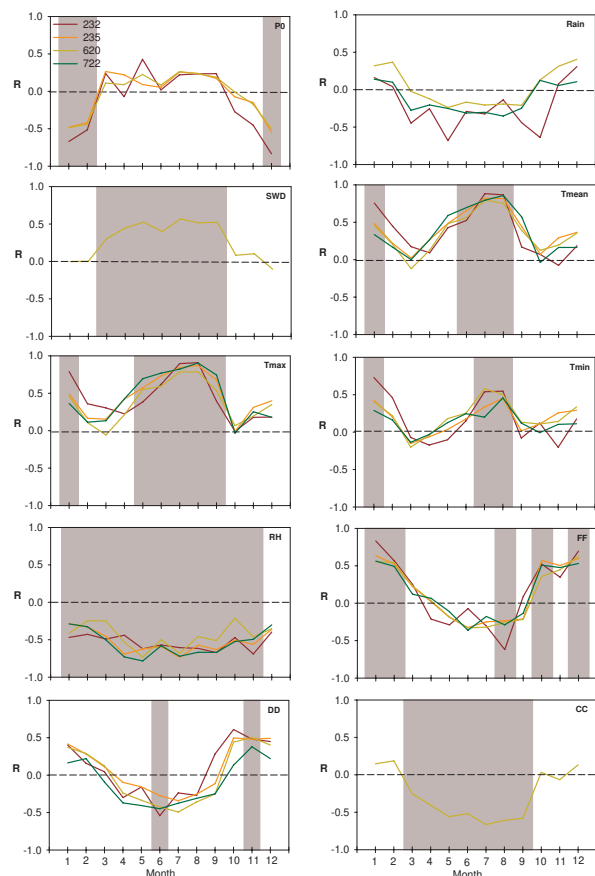


**Fig. 5.** Monthly mean Pearson correlation coefficients between daily maximum 8-hourly mean O<sub>3</sub> and all available meteorological variable anomalies for Volkel (232), Woensdrecht (235), Cabauw/Zegveld (620) and Hupsel (722). Correlation coefficients significant on the 99% level are depicted by the grey shaded area. Meteorological variables abbreviations are denoted in Sect. 2.1.

to investigate such hypothesis we have included in the analysis all meteorological values registered with 6, 12, 18, 24 and 48-h lag period (not shown). Below, results obtained for O<sub>3</sub> and PM<sub>10</sub> are described separately.

**O<sub>3</sub>** – In general, O<sub>3</sub> correlations are not responding differently on the different time lags. Only for the 12 and 18-h time lag, correlations coefficients between O<sub>3</sub> and SWD changes from positive to negative values. This is due to daily cycle of the radiation terms at mid-latitudes, which changes from a positive sign during daytime to a negative sign at night. The annual cycle of the correlations coefficients for temperature show a similar response as for SWD (Fig. 5), with a strong positive correlation between O<sub>3</sub> and Tmean/Tmax (with  $R=0.89/0.91$  respectively) in summer. This response is the opposite of that found for cloud cover, with strong negative correlations in summer. Over the whole year, O<sub>3</sub> is significantly negatively correlated with relative humidity. During summer (JJA), O<sub>3</sub> concentrations are negatively cor-

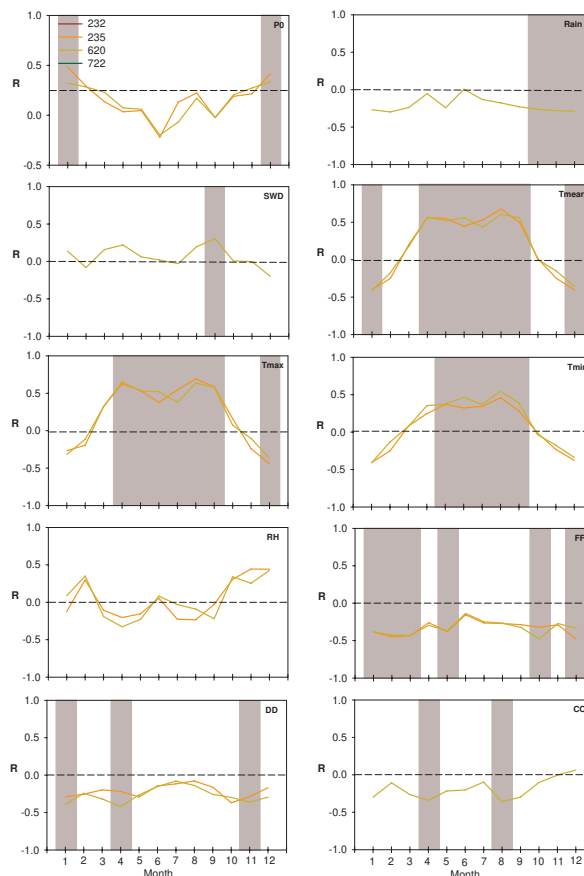


**Fig. 6.** As in Fig. 5, but for PM<sub>10</sub> and the stations of Woensdrecht (235) and Cabauw/Zegveld (620) only.

related to wind speed, with a minimum of  $-0.61$ , whereas this signal reaches a maximum of  $0.83$  in winter (DJF). This dichotomy is in good agreement to the results of Davies et al. (1992), who found similar correlations between a wind speed index and O<sub>3</sub> concentrations measured in Cabauw for the period 1978–1988 (see their Fig. 4). Another striking effect is the significant negative correlation between sea level pressure and O<sub>3</sub> in winter. Together with the significant positive correlations of wind speed for this season, this could point to a transport of ozone from the lower troposphere due to tropospheric folding, as described by Davies et al. (1992) and Delcloo and De Backer (2008).

**PM<sub>10</sub>** – In general, correlations between PM<sub>10</sub> and meteorological variables on different time lags weaken as a function of an increasing time lag. Only the correlation coefficients for both the radiation variables swap sign in the course of the year, with a peak difference in summer, when solar radiation is the highest at these mid-latitude locations. The response of air temperature on PM<sub>10</sub> varies seasonally (Fig. 6), with the highest positive correlation coefficients during the JJA ( $0.69$ ), and negative during DJF ( $-0.44$ ). This is consistent with the results of van der Wal and Janssen

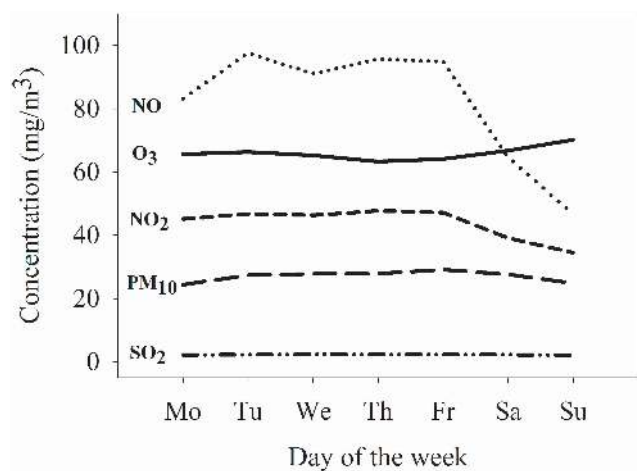


**Fig. 7.** Weekly cycles for O<sub>3</sub>, NO, NO<sub>2</sub> and SO<sub>2</sub> and PM<sub>10</sub> concentrations derived from the measurement station of Cabauw.

(2000), who found that higher PM<sub>10</sub> concentrations in winter (summer) coincide with lower (higher) temperature for PM<sub>10</sub> levels in the Netherlands. For relative humidity, there is an insignificant correlation throughout the year, whereas this correlation is systematic negative for daily precipitation, although the correlation coefficients are only significant for the months October, November and December. Similar to O<sub>3</sub>, wind speed is significant negative correlated to PM<sub>10</sub> for large parts of the year.

Previous research introduced a weekly cycle index as an additional variable in forecasting a) pollutant levels for the Athens area (Ziomas et al., 1995; Grivas and Chaloulakou, 2006), b) PM<sub>10</sub> levels in the Volos (Greece) area (Papanastasiou et al., 2007) or c) PM<sub>10</sub> values for Belgium (Hooybergs et al., 2005). However, in our case a weekly cycle is not well established for most pollutants with the exception of NO<sub>x</sub>, that shows a decrease during weekends (Saturday and Sunday) (Fig. 7). The fact that all measurement stations are denominated as rural, can explain why the day-of-the-week influence on the short-term variability is small. Flemming et al. (2005) confirms this limited weekly variation in O<sub>3</sub>, NO, SO<sub>2</sub> and PM<sub>10</sub> concentrations for German rural measurement stations. Furthermore, a weekly cycle characterised by the decreasing of NO<sub>x</sub> and corresponding increasing of O<sub>3</sub> during the weekend suggests that this is a NO<sub>x</sub> limited system (Reis et al., 2000).

In general, this analysis between the meteorological and air quality relationships shows only minor differences among the four different rural measurement sites considered within the Netherlands. These results appear to confirm those obtained by previous authors showing that rural areas can be considered as spatially homogeneous in terms of air quality concentrations (e.g. de Arellano et al., 1993; Flemming et al., 2005). Taking these facts into account we opt to carry on our analysis with Cabauw data only. Nevertheless, as cor-

relation coefficients between meteorological and air quality variables do not provide any information on the slope of the linear relation, a simple test is performed for these meteorological variables available for more than one station (not shown). The linear relations between meteorological and air quality variables reveal similar slopes in terms of sign and in terms of the slope an overall deviation in magnitude lower than 0.05. Hence, we consider the Cabauw station to be representative for rural areas in the Netherlands, a decision that is further supported by the fact that, unlike the others, this station has a comprehensive set of both meteorological and air quality variables.

Furthermore, the lag analysis also points out that the addition of time lags shorter than 1 day does not provide sufficiently additional information. Therefore, only the 1 and 2 day time lags for both meteorological and air quality variables are taken into account in the subsequent regression analysis. Finally, as mentioned before and shown in Fig. 7, a weekly cycle in air quality measurements from Cabauw is not well established; therefore, this variable is also dismissed.

#### 4.2 Stepwise multiple regression

A large amount of research has been conducted in the last decade to test the capacity of (linear) multiple regression (MLR) analysis and (non-linear) neural networks for air quality prediction purposes based on both air quality and meteorological input. It has been shown that model errors decrease by including persistency (lag effect) of the air quality variables (Perez et al., 2000; Smith et al., 2000; Perez, 2001; Barrero et al., 2006; Grivas and Chaloulakou, 2006). The aim of this research is to develop an approach that is also useful for downscaling operational low-resolution or AOGCM output data in terms of air quality assessment on the longer time scales. In this context, there is no information on the future air quality data and emissions as a dependent predictor variable. Therefore, the regression analysis is performed for two sets of predictors, both using measurements from Cabauw only: 1) without any air quality data, hereafter called MET, and 2) with the 24- and 48-h time lag values of air quality variables included as independent variables, hereafter called METCHE.

Table 2 shows the resulting model coefficients for both O<sub>3</sub> and PM<sub>10</sub>. All the variables introduced in the model are associated to a coefficient that is statistically significant. For both MLR<sub>MET</sub> and MLR<sub>METCHE</sub>, relative humidity is the most significant variable. This is in accordance with similar results using MLR for the prediction of ozone in four locations in Taiwan (Lu et al., 2006) and based on PCA for the region of Oporto in Portugal (Sousa et al., 2007). Furthermore, T<sub>max</sub> plays an important role, both on the present and previous day in both analyses for O<sub>3</sub>. Including air quality variables as predictors explains 15% more of the observed O<sub>3</sub> variance, whereby O<sub>3</sub> and NO<sub>2</sub> concentrations from the previous day



**Table 2.** Summary of the model coefficients *b*, the standardized coefficients  $\beta$  and *t*-statistic (indicating importance of the variable in the model) for the stepwise multiple regressions MLR<sub>MET</sub> and MLR<sub>METCHE</sub> for O<sub>3</sub> and PM<sub>10</sub>.

O <sub>3</sub>							
Variable	MLR <sub>MET</sub>			Variable	MLR <sub>METCHE</sub>		
	<i>b</i>	$\beta$	<i>t</i>		<i>b</i>	$\beta$	<i>t</i>
(Constant)	-0.60		-1.51	(Constant)	-0.59		-1.60
RH	-0.80	-0.30	-9.59	RH	-0.68	-0.26	-8.56
Tmax	1.52	0.26	6.79	O <sub>3</sub> (lag24)	0.36	0.36	14.73
P0 (lag24)	-0.32	-0.14	-5.89	Tmax (lag24)	1.39	0.23	7.38
SWD	0.06	0.16	5.072	NO <sub>2</sub> (lag24)	-0.17	-0.14	-4.62
Tmax (lag24)	0.82	0.14	4.36	SWD	0.054	0.15	4.97
FF	1.37	0.13	4.79	O <sub>3</sub> (lag48)	-0.12	-0.12	-5.14
DD (lag24)	0.19	0.066	2.60	P0 (lag24)	-0.30	-0.13	-5.60
Tmin	-0.65	-0.103	-2.65	Tmax	1.047	0.18	4.91
SWD (lag24)	0.021	0.058	2.20	Tmin (lag24)	-0.53	-0.081	-2.60
DD	0.012	0.056	2.048	FF	1.26	0.12	4.54
				FF (lag 24)	-1.18	-0.11	-3.85
				DD	0.022	0.076	3.29
				Tmin	-0.58	-0.089	-2.48
				NO (lag24)	-0.023	-0.072	-2.42
Calibration <sup>a</sup>							
R <sup>2</sup> (%)	37.0				52.0		
RMSE	14.25				12.75		
PM <sub>10</sub>							
Variable	MLR <sub>MET</sub>			Variable	MLR <sub>METCHE</sub>		
	<i>b</i>	$\beta$	<i>t</i>		<i>b</i>	$\beta$	<i>t</i>
(Constant)	1.08		2.49	(Constant)	0.91		2.059
FF	-1.48	-0.18	-4.54	PM <sub>10</sub> (lag24)	0.34	0.34	9.57
Tmax	1.34	0.29	7.57	NO (lag24)	0.037	0.16	3.85
SWD	-0.048	-0.19	-3.91	RH	0.44	0.23	4.84
FF (lag24)	-1.29	-0.17	-4.18	Tmax	1.10	0.23	6.024
CC (lag48)	-0.81	-0.12	-3.36	FF (lag24)	-1.28	-0.17	-3.83
Rain	-75.16	-0.15	-3.94	RH (lag24)	-0.19	-0.097	-2.42
RH	0.32	0.17	3.62	Rain	-65.45	-0.12	-3.23
DD (lag24)	-0.24	-0.11	-3.01	SWD	-0.032	-0.12	-2.71
Rain (lag24)	-40.81	-0.08	-2.27	NO (lag48)	0.018	0.081	2.23
				DD (lag24)	-0.016	-0.075	-2.006
Calibration <sup>b</sup>							
R <sup>2</sup> (%)	25.0				42.0		
RMSE	11.05				10.12		

<sup>a</sup> Calculated over the period 2001–2004<sup>b</sup> Calculated over the period 20/03/2003 to 31/12/2004

provide additional relevant information in agreement with results obtained in previous studies by Davis and Speckman (1999) and Barrero et al. (2006). Both MLR<sub>MET</sub> and MLR<sub>METCHE</sub> also reflect the importance of shortwave downward radiation and wind speed, and for MLR<sub>METCHE</sub>, the concentrations of nitrogen oxides on the previous day.

For PM<sub>10</sub>, wind speed is most significant when no air quality predictors are included while Tmax is important in both models, results that agree with those obtained by Stadtlober et al. (2008) for Bolzano (South Tirol - Italy). The model re-

sults improve from  $R^2=25.0$  for MLR<sub>MET</sub> to  $R^2=42.0$  when the air quality variables are included (MLR<sub>METCHE</sub>). Here, the previous day PM<sub>10</sub> concentration is shown to be an important parameter for the prediction of PM<sub>10</sub> levels, as was shown in previous works (e.g. Hooyberghs et al., 2005; Stadtlober et al., 2008). Furthermore, also previous day NO is an important indicator for high PM<sub>10</sub> concentrations. This strong correlation indicates road traffic as a local source (Harrison et al., 1997). Although Cabauw/Zegveld is classified as a background rural station, the different behavior of

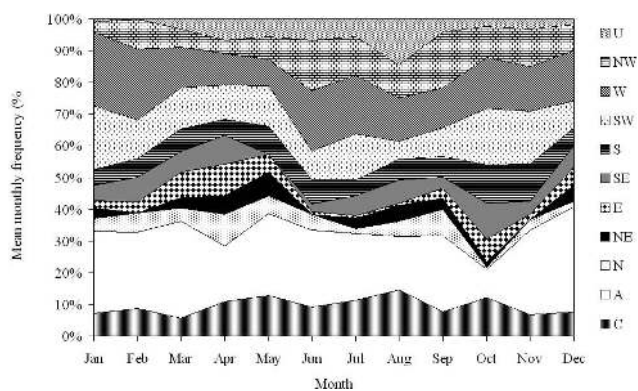


**Fig. 8.** Monthly mean frequencies of Lamb Weather Types over the period 2001–2004. The acronyms of circulation patterns are as follows: U=unclassified, NW=northwest, W=West, SW=southwest, S=south, SE=southeast, E=east, NE=Northeast, N=North, C=Cyclonic and A=Anticyclonic.

NO depending on the day of the week (Fig. 4) points to a possible influence of road traffic on the PM<sub>10</sub> measurements. This tendency is confirmed by the recent results of Schaap et al. (2008), who have found higher PM<sub>2.5</sub> concentration in Cabauw compared to other European rural background areas. A comparison of the quality of the two models for PM<sub>10</sub> shows that our results are of similar magnitude of those by Slini et al. (2006) and van der Wal and Janssen (2000), that have obtained a correlation coefficient of respectively 29.7 and 25.0% without any further information on air quality predictors. In the following Sect. 5, a more thorough validation of the MLR approach and a comparison with the circulation approach will be performed.

### 4.3 Circulation-to-environment approach

The interannual variability of the eleven resulting Weather Types (WTs) is depicted in Fig. 8, showing the relative frequency of each WT averaged for each month over the period 2001–2004. The anticyclonic type is the most frequent circulation pattern throughout the year, except for the month of October, which is dominated by the southwest (SW) and west (W) circulation types. Throughout the year, the relative frequency of cyclonic situations is almost constant, reaching a peak in August. The meridional circulation types north (N) and south (S) are rather constant throughout the year, except for a decrease of N observable from October to December. All WTs with a westerly component and thus originating in the Atlantic Ocean (SW [southwest], W [west], NW [northwest]) present stable relative frequencies through most of the year, although the NW regimes decline during winter and early spring. This phenomenon is counteracted by an increase of anticyclonic types between March and May, which is in agreement with the well known maximum of blocking frequencies over the Euro-Atlantic region (d'Andrea et al.,

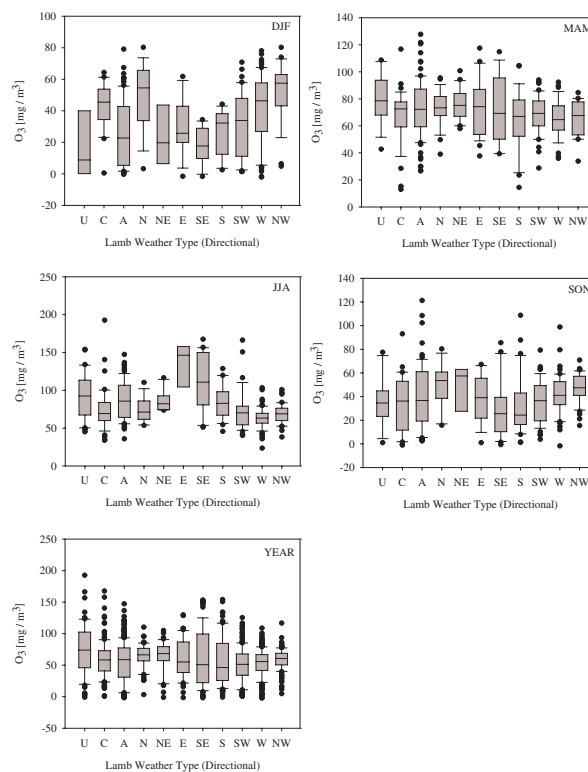


**Fig. 9.** Box – Whiskers plots with the concentrations of O<sub>3</sub> according to the Lamb weather type classes per season and year, averaged over the period 2001–2004. The box and whiskers present the median, the first and third quartiles, the minimum and maximum value and possible outliers. The circulation types are the same as in Fig. 8.

1998; Trigo et al., 2004). The remaining types with an eastern component (NE, E [east] and SE [southeast]) are the least frequent of all weather types throughout the year with the relative frequencies of E being virtually zero between May and August.

The analysis in Sect. 2.3 (Fig. 3) has shown that the annual distribution of O<sub>3</sub> and PM<sub>10</sub> is similar over the various rural sites in the Netherlands. Therefore, the circulation type-specific O<sub>3</sub> and PM<sub>10</sub> concentrations are analysed for the Cabauw measurement site only. Figures 9 and 10 depict the statistical distribution of O<sub>3</sub> and PM<sub>10</sub> according to their respective WT class. Because some weather type clusters have insufficient data, a few percentile bars/outliers are absent from Fig. 10. For O<sub>3</sub>, an insignificant explained variance (0.03) and  $\alpha_{KW} > 1\%$  show a limited discriminative power over the whole year (Fig. 9). Nevertheless, the results based on seasons show some significant results. For DJF, highest concentrations can be observed in the C (Cyclonic), N, W and NW WTs. Davies et al. (1992b) obtained similar dependence for ozone with N, NW and W weather patterns in Cabauw. It is noticed that some of the latter

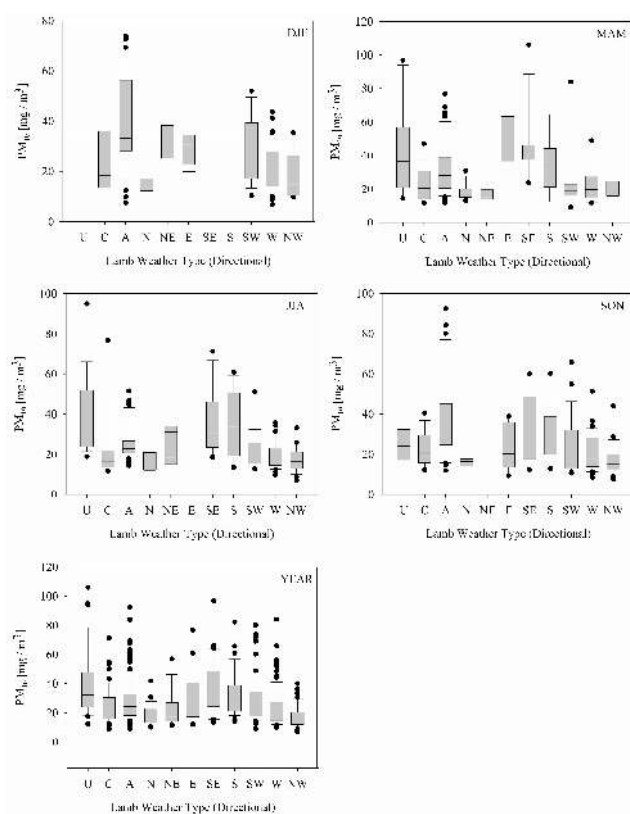


**Fig. 10.** As in Fig. 9, but for PM<sub>10</sub>.

are related to strong winds and tropopause folding mechanisms whereby ozone can be transported from the lower troposphere (Delcloo and De Backer, 2008). The lowest DJF concentrations can be found in E, SE and S directional circulation patterns. This discriminative power of the WT technique for O<sub>3</sub> assessment is supported by an explained variance of 26.0% and  $\alpha_{KW} < 1\%$ . Lamb weather types do not succeed in explaining a great deal of the observed variance in MAM, which is also supported by an insignificant  $R^2$  factor (5.0%) and  $\alpha_{KW} > 1\%$ . The relation between the WTs and concentration of O<sub>3</sub> in JJA is opposite compared to the DJF situation. Whereas in DJF the highest concentrations are found in West to North directions, in JJA these can be found in opposite East-Southeast directions. This coincides with the highest median concentrations of NO and NO<sub>2</sub> for the SE circulation pattern (not shown). This increased transport of NO<sub>x</sub> in summer from the densely populated Ruhr area (located south-easterly) makes the atmosphere more abundant of O<sub>3</sub> precursors, which can lead, in combination with positive temperature anomalies/increased solar radiation, to higher O<sub>3</sub> formation and concentrations. The SON patterns are typical of a transitional period characterised by changing conditions from JJA to DJF, namely with a shift in highest concentrations from North to Easterly directions, and lower concentrations from Southeast to Southerly directions. For

both JJA and SON,  $\alpha_{KW} < 1\%$ , so that the medians of the O<sub>3</sub> and PM<sub>10</sub> clustered per weather type group are significantly different.

In general, the Kruskal-Wallis test shows that the Lamb weather types are able to distinguish between high and low episodes of PM<sub>10</sub>, with  $\alpha_{KW} < 1\%$  in all seasons and over the whole year averaged. For DJF, the Box-Whisker plot shows the lowest concentrations of PM<sub>10</sub> originating from Western to Northern circulation patterns, and the highest median concentrations during A and SE WTs. This is supported by the findings of van der Wal and Janssen (2000) who has obtained the highest PM<sub>10</sub> levels in DJF in the Netherlands with winds prevailing from east to southeast. The explained variance is the highest (30.0%) when compared to the other seasons. In MAM, the highest PM<sub>10</sub> concentrations are grouped with the WTs ranging from East to South directions, which could be associated to the transport of PM<sub>10</sub> from the high industrial Ruhr area. As for DJF and MAM, the highest PM<sub>10</sub> levels can be found for the SE and S classes, and the lowest levels for types originating from West to Northwest. Again, this confirms the results of van der Wal and Janssen (2000) who reported higher levels of PM<sub>10</sub> in JJA during dry weather condition with positive temperature anomalies, which is the case for the SE and S Lamb weather types (not shown). In autumn, the explained variance is the lowest (21.0%), although the highest levels of PM<sub>10</sub> can again be associated with southeast to southern flow patterns.

In order to gain further insight into the physical conditions behind the WT-air quality relationships, we derive the seasonal composite pressure maps for each circulation pattern that is associated with the highest median of O<sub>3</sub> and PM<sub>10</sub> (Figs. 11 and 12). For each season, the circulation type with the highest median of the air quality variable is identified, and the corresponding mean circulation pattern is depicted for the period 2001–2004 together with the MSLP, temperature and relative humidity anomalies (computed with the normal period from 1971–2000). For O<sub>3</sub>, the winter surface MSLP composite map shows a meridional pressure gradient, with high pressure located just west of Ireland, and a low-pressure system positioned over North-Eastern Europe. This implies a strong northerly circulation that is consistent with previous results of a strong correlation between high O<sub>3</sub> levels and strong winds in winter (Davies et al., 1992b). The anomaly maps show an enhanced positive pressure anomaly south of Iceland, and a negative anomaly east of Cabauw. These patterns also suggest strong winds and high frequencies of troughs or even cut-off lows in the vicinity of the observation station, which suggests transport of air mass from the upper troposphere (low troposphere) to the surface (Delcloo and De Backer, 2008). This could explain the higher concentrations associated with these patterns, as in non-summer months there is less opportunity for photochemical production of ozone in the boundary layer (Davies et al., 1992b).

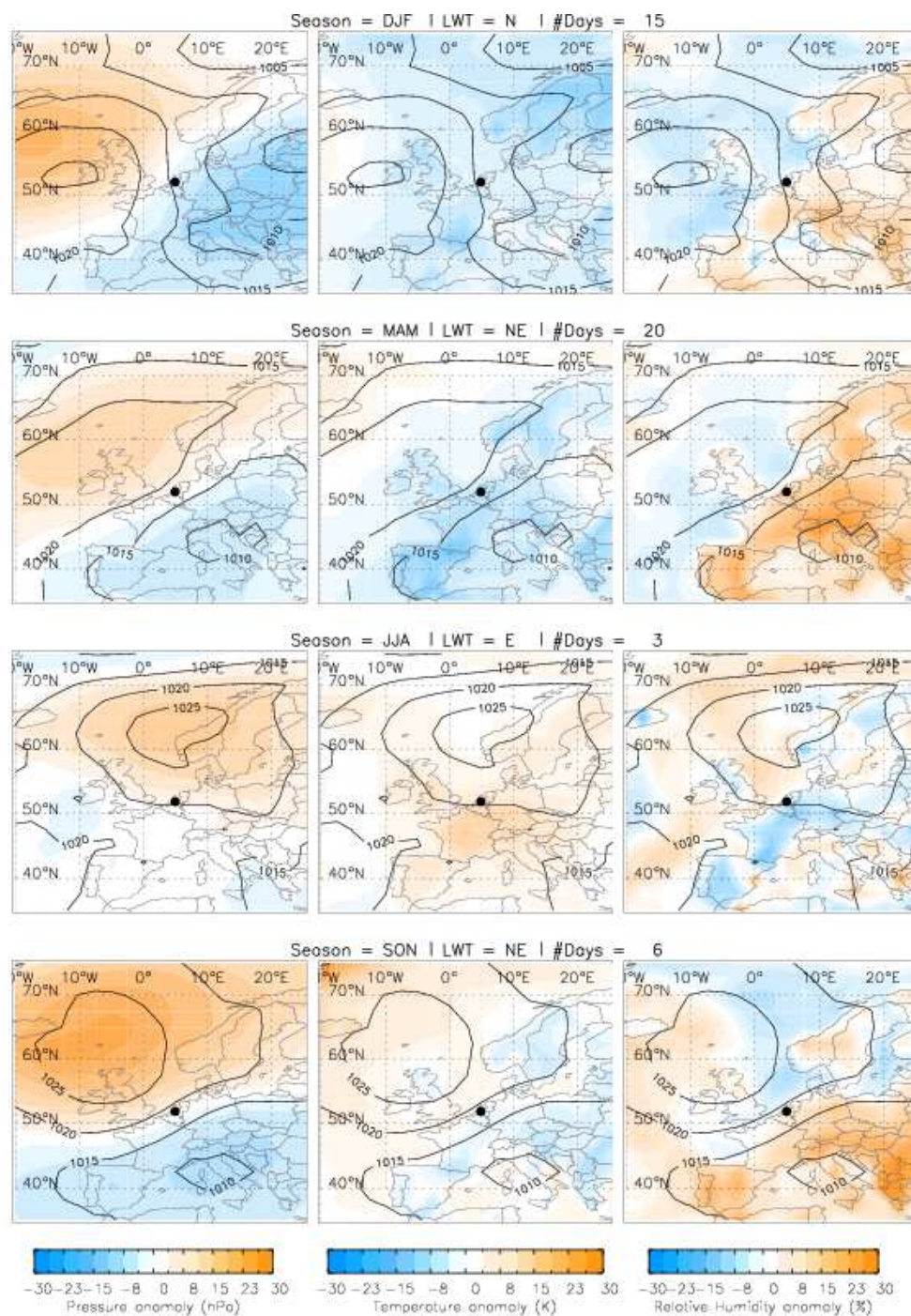


**Fig. 11.** Mean surface pressure fields (in hPa) for the circulation type in each season characterized by the highest median O<sub>3</sub> concentration for the period 2001–2004. Shaded colors show the pressure anomalies (left panels), 2 m temperature anomalies (middle panels) and relative humidity anomalies (right panels) from the long-term mean (1971–2000). The full dot refers to the Cabauw measurement location.

The spring MSLP maps show the Azores high pressure system extending far towards the northeast and a low located over Italy. This pattern results in a weak northwest-southeast pressure gradients and resulting winds from the northeast and a negative (positive) temperature (relative humidity) anomaly

over continental Europe. The spring MSLP anomalies indicate that the pressure gradient is slightly stronger than normal, a fact that is consistent with the positive (albeit insignificant) relation with wind speeds in spring.



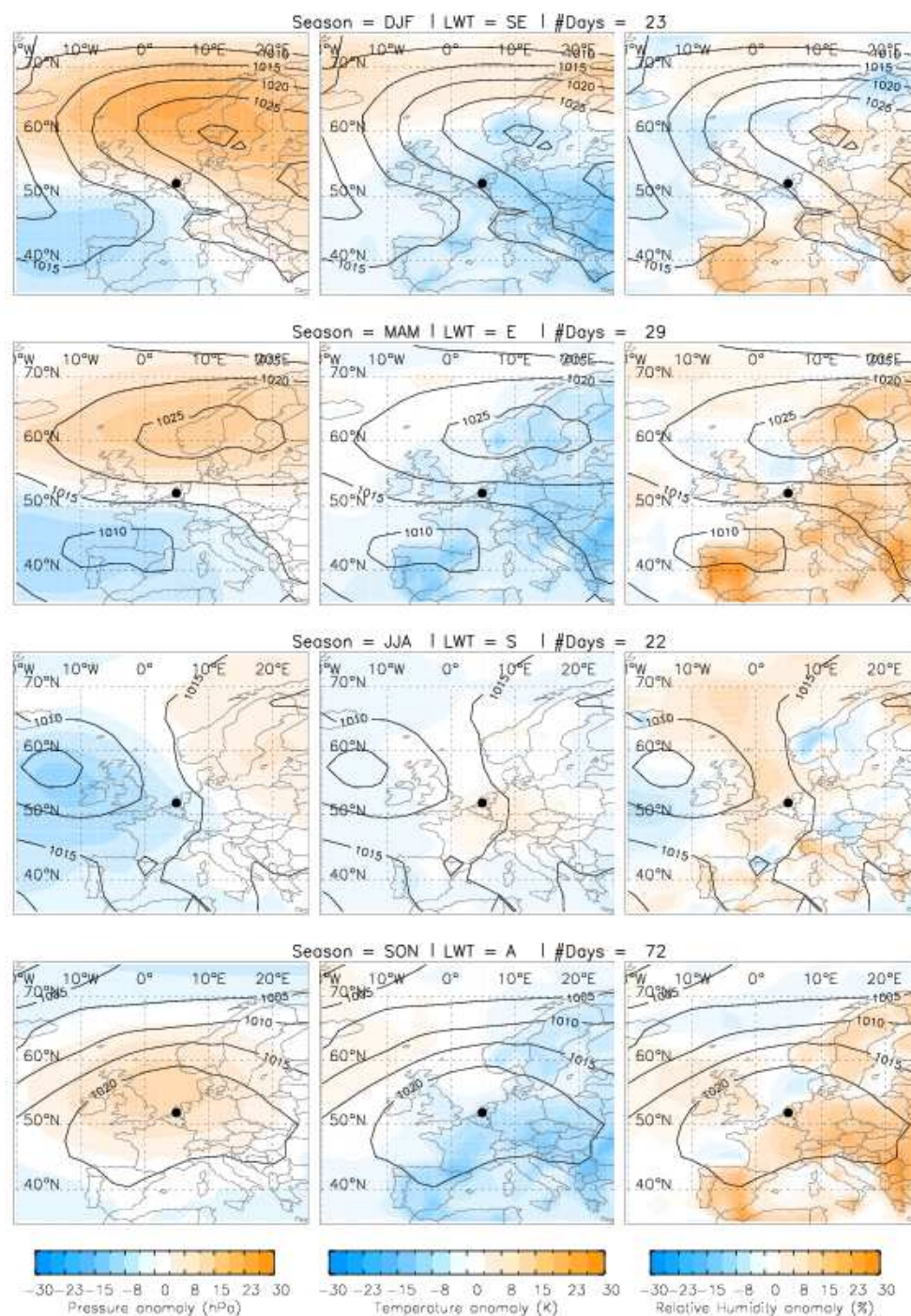


**Fig. 12.** Same as Fig. 11, but for PM<sub>10</sub>.

The JJA composite MSLP maps show a strong anticyclonic system located north of Cabauw, resulting in a weak meridional flow. This situation transports warm and dry air from east and central Europe to large parts of Western Europe promoting the appearance of a positive (negative) temperature (relative humidity) anomaly fields. This is consistent with the strong positive (negative) relation between tem-

perature (relative humidity) that characterises high O<sub>3</sub> levels in summer. Pressure gradients and corresponding anomalies are generally weak, which is also consistent with the negative relationship between high O<sub>3</sub> levels and wind speed. These findings confirm the results of Delcloo and De backer (2008), who have shown that high summer ozone events in Uccle (Belgium) – which has generally similar synoptic

characteristics as Cabauw – are often generated by slow moving air masses, residing over the continent. Furthermore, our results agree with those of Guicherit and Van Dop (1977), who found a similar relation in the 1970s between high ozone levels and the synoptic situation above the Netherlands. The Grosswetterlagen patterns (Baur et al., 1944; Hess and Brezowsky, 1952) associated with their high ozone levels events describe a closed high over Middle Europe (HM), high over Scandinavia (Hfa) or high over the North Sea – Iceland (Hna), comparable to our results using Lamb weather types.

The autumn composite MSLP map exhibits a strong northwest-southeast pressure gradient, with an enhanced flow from the northeast. A positive pressure anomaly located northeast of the British Isles presents the highest magnitude when compared to those obtained in other seasons. Anomalies for temperature and relative humidity are generally characterised by negligible values which consistent with our explorative correlation analysis in Sect. 4.1.

For PM<sub>10</sub>, high levels occur during those occasions where air masses are advected from the south or east. In DJF, a large anticyclonic system covers large parts of north and Eastern Europe, associated with a high positive pressure anomaly centred west of the Norwegian coast. Such pattern results in a south-eastern flow (over the highly industrialized Ruhr area), and advection of cold continental air. This is consistent with the negative correlation of PM<sub>10</sub> levels with temperature and mean sea level pressure (Sect. 4.1) and the results obtained by van der Wal and Janssens (2000), who have used PM<sub>10</sub> data of nineteen monitoring sites in the Netherlands (for the period 1993–1994). In MAM, this pattern is similar, although weaker, with a positive anticyclonic system placed over Scandinavia, and a low pressure placed over the Bay of Biscay, again advecting cold air from central Europe. In summer, pressure gradients are generally weaker, with a small negative (positive) pressure anomaly located west of Ireland (Baltic Sea) promoting the advection of warm air from the south. A result that is consistent with the positive correlation of PM<sub>10</sub> levels and wind speed in JJA, confirming the results obtained by van der Wal and Janssen (2000) who stated that concentrations of PM<sub>10</sub> are higher than normal during summer under conditions of high temperatures and dry weather. Autumn is characterised by a blocking high-pressure system over the northern sea, which results in calm, colder than normal weather over the area.

## 5 Validation of MLR and LWT

In the previous Sect. 4.2 and 4.3 we have derived results for the MLR and WT approaches highlighting the resemblance with similar research done for Benelux and in other regions. Here we provide an objective comparison between the results obtained with the MLR and the WT air quality assessment models, using the period 2001–2004 for calibration and the remaining years 2005–2006 for validation purposes. For

MLR, the regressions obtained in Sect. 4.2 are used on the validation dataset while for the WT methodology, O<sub>3</sub> and PM<sub>10</sub> means are computed for each of the circulation patterns for 2005–2006. The average value of the air quality variable associated with each circulation pattern is used to reconstruct the time series.

Results achieved with all the developed models, for both the calibration and validation periods, are shown in Table 3. In general, MLR techniques are known to underestimate peak levels of ozone (Barrero et al., 2006). Interestingly, although the MLR model is built using the calibration dataset only, we can observe an increase in accuracy for O<sub>3</sub> (>10% in explained variance) when the model is applied to the validation dataset for both MLR<sub>MET</sub> and MLR<sub>METCHE</sub>. Thus, errors between observed and modelled O<sub>3</sub> levels from the validation period decrease (while  $R^2$  increases), especially in JJA and DJF with 15% and 30% respectively. In terms of seasonal differences, the regression model explains more of the observed variance in DJF and JJA and less in the transition seasons. The skill score against the climatological mean is higher than 90% for both MLR<sub>MET</sub> and MLR<sub>METCHE</sub>, which points out that a forecast based on climatology is easily outperformed by a linear model (or an analysis based on circulation patterns). As expected, persistence corresponds to a benchmark model considerably more difficult to beat, therefore any positive values of SSp are particularly relevant. The better quality of the MLR<sub>METCHE</sub> model when compared with the MLR<sub>MET</sub> can be observed in this assessment against persistence, with an improved skill score from 36 to 50% (validation period) and from 9.9 to 27% (validation period) for MLR<sub>MET</sub> and MLR<sub>METCHE</sub> respectively.

Table 3 also reveals an improvement for the WT approach applied on the validation dataset compared to the calibration dataset. In general, the circulation patterns explain less than 21% of the observed O<sub>3</sub> variance, again with the highest scores being observed in DJF and JJA. Explained variance improves significantly (between 10 to 16%) for the WT based on seasonal means compared to yearly averages. However, overall scores are considerably lower when compared to those obtained with MLR while the RMSE values are about 5  $\mu\text{g}/\text{m}^3$  higher compared to those from the regression analysis. Although WT presents a good skill score against the climatological mean, it fails to show any significant improvement against persistence, revealing sometimes even a lower quality than the persistence model. These results implies that, although circulation patterns are able to discriminate between high (low) concentrations for different seasons and WTs, day-to-day variability and the complex sequence of physic-chemical ozone formation/destruction mechanisms play a large role that can not be fully captured by the circulation pattern classification.

For PM<sub>10</sub>, the performance of the model improved significantly for MLR<sub>MET</sub> model, with a  $R^2$  increase of 25 and 35% for the calibration and the validation periods respectively. However, the MLR<sub>METCHE</sub> reveals a slight decrease in



**Table 3.** Validation of the multiple linear regression in 2 modes (MLR-MET and MLR-METCHE) and the Lamb weather type approach in 2 modes (LWT-year and LWT-seas) using the explained variance ( $R^2$ ), root mean square error (RMSE) and two skill scores (SSc and SSp) for O<sub>3</sub> and PM<sub>10</sub> over the whole measurement period and the validation period 2005–2006. Insignificant values (on the 95% level) are denoted with \*.

<i>Calibration (2001–2004)</i>		$R^2$ (%)				RMSE	SSc	SSp
	Year	DJF	MAM	JJA	SON			
<i>O<sub>3</sub></i>								
MLR-MET	37.2	29.2	36.0	50.4	33.6	15.1	94.6	36.3
MLR-METCHE	51.8	50.4	43.6	60.8	44.9	13.3	95.8	50.4
LWT-year	1.2	3.24	3.61	8.41	0.00*	19.0	91.4	−0.95
<i>LWT-seasonal</i>	12.3	5.29	5.76	22.1	4.84	17.9	92.4	10.7
<i>PM<sub>10</sub></i>								
MLR-MET	25.0	23.0	26.0	28.1	24.0	12.1	72.8	16.9
MLR-METCHE	42.3	31.4	50.4	36.0	46.2	10.7	86.3	34.5
LWT-year	13.0	12.3	17.6	16.0	9.61	12.9	80.1	4.59
<i>LWT-seasonal</i>	17.6	17.6	22.1	18.5	16.8	12.6	81.1	9.63
<i>Validation (2005–2006)</i>								
<i>O<sub>3</sub></i>								
MLR-MET	51.8	64.0	38.4	68.9	26.0	11.3	96.8	9.90
MLR-METCHE	62.4	65.6	51.8	77.4	28.1	10.1	97.4	28.0
LWT-year	4.0	0.09*	1.69	13.0	0.49*	15.7	93.7	−73.8
<i>LWT-seasonal</i>	20.9	23.0	6.25	29.2	0.16*	14.2	94.8	−43.3
<i>PM<sub>10</sub></i>								
MLR-MET	34.8	21.2	51.8	44.9	32.5	6.06	78.3	1.18
MLR-METCHE	36.0	27.0	46.2	51.8	30.3	6.24	93.4	−4.58
LWT-year	15.8	16.8	24.0	21.2	7.84	6.74	92.2	−22.2
<i>LWT-seasonal</i>	23.3	22.1	27.0	24.0	20.3	6.44	92.9	−11.3

performance from 42% to 36% between these two datasets. In general, the overall best performance (based on  $R^2$ ) is obtained in MAM, JJA and SON, depending if the air quality variables are included as predictors or not. Results are worse for DJF, which could be due to possible high PM<sub>10</sub> events related to an increased surface stability (surface inversion) that is not captured by MLR trained with surface meteorological data. The skill score for the calibration and validation dataset against climatology improves 15% for both periods, between the MLR<sub>MET</sub> and MLR<sub>METCHE</sub>. The skill score against persistence improves similarly for the calibration dataset, although this is not the case for the validation dataset.

The analysis for the PM<sub>10</sub>-LWT approach shows low coefficients for  $R^2$ , although somewhat higher compared to the  $R^2$  obtained for the O<sub>3</sub>-LWT model, with a maximum explained variance for the validation period using LWT based on seasonal averages ( $R^2=23.29$ ). Identical to MLR, the observed variance for PM<sub>10</sub> is explained the most in MAM, and JJA. The skill score against climatology is higher for both the calibration and validation dataset compared to the MLR<sub>MET</sub>, with overall high scores (>80%). For the calibration dataset, the LWT approach is performing slightly better than the per-

sistence model, while for the validation dataset, results are worse.

Concerning the WT classification method, it is fair to state that our results partially contradict previous studies that discussed the strength of synoptic categories in relation with air pollution concentrations (e.g. Comrie and Yarnal, 1992; Davies et al., 1992b; Kalkstein et al., 1996; Cheng and Lam, 2000; Ainslie and Styen, 2007). This discrepancy could be due to multiple reasons. However, we firmly believe that the most important reason is associated with the lack of validation measures used in those studies. In fact these studies described synoptic situations associated with characteristic levels of an air quality variable without objectively quantifying this result, an approach that can lead to misleading results. Nevertheless other issues may also intervene, as for e.g. levels of air pollutants associated with typical circulation patterns are solely compared to other classification approaches (Cannon et al., 2002). Furthermore, there are many different classifications techniques of atmospheric circulation types (PCA, clustering, etc) taking into account a different number of variables on various pressure levels (Huth et al., 2008) and their use could alter our findings to a certain degree.

In summary, our statistical analysis reveals that the single use of a weather type approach is limited in terms of short-term day-to-day air quality forecasts. Nevertheless, our analysis also shows that a circulation type approach brings forward some interesting physical relations between large-scale circulation patterns and associated air quality concentrations. This supports the use of this approach with respect to future long-term air quality projections and low temporal air quality fluctuations, as was recently successfully tested for PM<sub>10</sub> at several Bavarian sites in Germany (personal communication, C. Beck, 2008).

## 6 Summary and conclusion

We investigate the relationships of climatology and air quality by statistically analyzing meteorological and air quality variables calculated and observed at 4 rural sites in the Netherlands. On the one hand, interactions between meteorology and O<sub>3</sub> and PM<sub>10</sub> on the local-scale are quantified based on a multiple linear regression analysis, a technique often used in short-term air quality forecasts. On the other hand, the Lamb weather type circulation classification method is applied as an alternative air quality prediction tool. This technique is potentially useful as downscaling tool of future climate scenarios for local air quality purposes.

By selecting these methods, we seek simplicity, linearity and practical feasibility of the models in order to make this approach appropriate for downscaling forecasted meteorological fields or AOGCMs scenarios for air quality purposes. The multiple linear regression model guarantees simplicity, and applying the regression without (MLR<sub>MET</sub>) or with air quality variables (MLR<sub>METCHE</sub>) as predictors, provides a comprehensive summary on the capabilities of these 2 modes. Comparing the results of this local-meteorology based approach with results from a circulation point-of-view based on mean sea level pressure, which takes into account the large-scale circulation above our area of interest, provides further insight in the controlling processes forming and resulting in representative O<sub>3</sub> and PM<sub>10</sub> levels for rural midlatitude sites.

Prior to the construction of the multiple regression models, a comprehensive correlation study is conducted between all meteorological and air quality variables for all stations. The dataset is extended including all meteorological variables on a 6, 12, 18, 24 and 48-h time lag, in order to investigate any lagged effect on the meteorological-air quality relations. In general, this analysis shows a limited response of the air quality variables on the <1-day lag meteorological variables, apart from the inverse relations with downward solar radiation, explaining the day and night cycle. Furthermore, a clear relation is found between O<sub>3</sub> and (maximum) temperature in JJA, combined with a low relative humidity. Rain amount is significant negatively correlated with PM<sub>10</sub> in winter, which could point out atmospheric removal due to

wet deposition. Wind speed is strongly negative correlated with PM<sub>10</sub> over the whole year and with O<sub>3</sub> in winter, while this relation is positive during summer for the latter. Furthermore, this analysis shows that different rural sites for a similar mid-latitude area have similar characteristics, both in terms of the annual cycle of O<sub>3</sub> and PM<sub>10</sub> as in their relation with the suite of selected meteorological variables. This provides confidence in the spatial homogeneous character of rural sites for a mid-latitude area in the Netherlands and justifies the use of a single rural station (with abundant air quality and meteorological measurements) for the remaining of this analysis.

Secondly, both multiple linear regression modes reveal promising results in forecasting especially O<sub>3</sub> for rural sites in the Netherlands, outperforming both climatology and persistence models. The input variables are selected in the way that they are available from operational forecast or AOGCM output (for the MET mode) and the simple and transparent character of the model provides clear insight in the importance of the specific variables that govern the evolution of O<sub>3</sub> and PM<sub>10</sub>. The statistical performance is good in comparison to similar statistical studies for both the calibration and the validation period, testing the 2 modes MLR<sub>MET</sub> and MLR<sub>METCHE</sub>. In general, including information on the previous-day air quality variables improves the explained variance with 10 to 18% for ozone and PM<sub>10</sub> respectively, with the best results for MLR<sub>METCHE</sub> for PM<sub>10</sub> in the calibration period (42.0%), and for ozone using MLR<sub>METCHE</sub> in the validation period (62.0%). Moreover, this performance is promising when considering the skill scores against persistence, with an improvement of almost 20% for some model situations.

In order to acquire a deeper understanding of the linear relations obtained, levels of O<sub>3</sub> and PM<sub>10</sub> are connected to large-scale circulation patterns using the objective Lamb weather type approach. Based on 12 h UTC operational analysis of MSLP extracted from ECMWF, eleven circulation types are obtained, being associated with levels of O<sub>3</sub> and PM<sub>10</sub> at the seasonal and annual scales. As shown by other authors in previous research, some clear physical links can be seen between the large-scale patterns and high (low) pollution events. As a general rule, most relations between pressure, wind speed, temperature and relative humidity and levels of O<sub>3</sub> and PM<sub>10</sub> found in our correlation analysis (using observations from all rural sites) can be retrieved independently using the seasonal composite circulation patterns and their associated anomalies. For O<sub>3</sub>, the surface pressure composite maps generally show an anomalous strong high located north or west from the measurement station, depending on the season. This results in cold and humid (DJF and MAM) and warm and dry (JJA) air advected from north to east wind directions, contributing to higher than normal ozone concentrations. Using the circulation patterns for ozone in winter reveals the highest average concentration in wind direction from W to N, under high wind speed

circumstances. This feature suggests the influence of ozone transported from the free troposphere towards the surface, which was also suggested by Davies et al. (1992b) and Delcloo and De Backer (2008). For PM<sub>10</sub>, high levels are largely controlled by air advected from the south to east. Hereby, pressure gradients are often low, with a positive pressure anomaly north- to eastwards from the measurement station, again depending on the season.

Finally, reconstructing the time series of O<sub>3</sub> and PM<sub>10</sub> for the calibration and validation period objectively compares the multiple stepwise regressions and the objective Lamb weather type approach. Although the explained variance and the skill score against climatology is high (>80%), the results against persistence can be rather poor, often revealing important structural weakness of the models. In this regard, the stepwise regression for O<sub>3</sub> performs satisfactory for all indices. Contrarily, although seasonal composite maps have shown a distinct pattern for typical episodes of high average O<sub>3</sub> and PM<sub>10</sub> concentrations, the Lamb weather type as an air quality forecast model performs poor for both O<sub>3</sub> and PM<sub>10</sub>, with the skill score against persistence being, in some situations, even worse than persistence itself. On the one hand, this result could be due to the short time availability of the air quality data, which restrains the possibility to obtain a robust dataset with significant within-season and type-associated differences in concentrations of O<sub>3</sub> and PM<sub>10</sub>. On the other hand, this result points out the limitation of the circulation-based approach in terms of day-to-day air quality forecasts. And although circulation patterns are not able to capture the short-term fluctuations of the pollutants, which is to be expected from the intrinsic nature of the circulation, this approach can provide a clear insight in typical large-scale atmospheric structures and associated anomalies in meteorological variables during high (or low) pollution events. We are confident that the multi model approach presented here can be used in other rural settings, particularly those located in mid-latitudes where several different weather type classifications have been developed and validated. Moreover, as this tool can easily be transferred to other geographical areas, it is a promising tool in discriminating atmospheric conditions leading to relatively low or high concentrations of O<sub>3</sub> and PM<sub>10</sub> (and probably other pollutants as well). In this respect, further research could provide more insight in the possible adaptation of the multiple regression results on AOGCM output, the use of circulation pattern in providing possible long-term trends of a specific air quality variable, and on the use of a combination of a combined multiple regression and circulation-type approach. Thereby, O<sub>3</sub> and PM<sub>10</sub> levels could be explained using the multiple regression technique for the local-scale photochemical formation and the circulation-based approach for the large-scale transport of (secondary) pollutants from other source areas.

*Acknowledgements.* This research is funded by a PhD grant of the Institute for the Promotion of Innovation through Science and Technology Flanders. The authors are especially thankful to the COST Office and the constructive discussions in the framework of COST action 733 on Harmonization and Applications of weather types Classifications for European Regions. RMT participation was supported by the Gulbenkian Foundation through project IMPACTE (No 1568). ECMWF is acknowledged for providing operational ECMWF data. Furthermore I gratefully thank Fred Bosveld from KNMI in providing the observations from the rural measurement sites and Hans Berkhout (RIVM) for his helpful insight information on the air quality measurements and locations. The manuscript has been improved by the careful reading and interesting suggestions of J. Dawson and an anonymous reviewer.

Edited by: R. Ebinghaus

## References

- Agirre-Basurko, E., Ibarra-Berastegi, G., and Madariaga, I.: Regression and multilayer perceptron-based models to forecast hourly O<sub>3</sub> and NO<sub>2</sub> levels in the Bilbao area, *Environ. Model. Softw.*, 21, 430–446, 2006.
- Ainslie, B. and Steyn, D. G.: Spatiotemporal trends in episodic ozone pollution in the Lower Fraser Valley, British Columbia, in relation to mesoscale atmospheric circulation patterns and emissions, *J. Appl. Meteor. Climatol.*, 46, 1631–1644, 2007.
- Al-Alawi, S. M., Abdul-Wahab, S. A., and Bakheit, C. S.: Combining principal component regression and artificial neural networks for more accurate predictions of ground-level ozone, *Environ. Model. Softw.*, 23, 396–403, 2008.
- Andersson, C. and Langner, J.: Inter-annual variations of ozone and nitrogen dioxide over Europe during 1958–2003 simulated with a regional CTM, *Water Air Soil Poll.*, 7, 15–23, 2007a.
- Andersson, C., Langner, J., and Bergström, R.: Interannual variation and trends in air pollution over Europe due to climate variability during 1958–2001 simulated with a regional CTM coupled to the ERA40 reanalysis, *Tellus A*, 59B, 77–98, 2007b.
- Barrero, M. A., Grimalt, J. O., and Canton, L.: Prediction of daily ozone concentration maxima in the urban atmosphere, *Chemometr. Intel. Lab. Sys.*, 80, 67–76, 2006.
- Baur, F., Hess, P., and H. Nagel, H.: *Kalendar der Groswwetterlagen Europas 1881–1939*, Bad Homburg, Germany, 1944.
- Beljaars, A. C. M. and Bosveld, F. C.: Cabauw data for the validation of land surface parameterization schemes, *J. Clim.*, 10, 1172–1193, 1997.
- Benvenuto, F. and Marani, A.: Nowcasting of urban air pollutants by neural networks, *Nuovo Cimento Della Societa Italiana Di Fisica C-Geophysics and Space Physics*, 23, 567–586, 2000.
- Bridgeman, H. and O'Connor, J.: Relationships between air pollution and meteorology in Newcastle, Australia, *Proceedings of the 6th international conference on Urban Air Quality*, 2007.
- Brunekreef, B. and Holgate, S. T.: Air pollution and health, *Lancet* 360, 1233–1242, 2002.
- Cannon, A. J., Whitfield, P. H., and Lord, E. R.: Synoptic map-pattern classification using recursive partitioning and principal component analysis, *Mon. Weather Rev.*, 130, 1187–1206, 2002.
- Cheng, S. Q. and Lam, K. C.: Synoptic typing and its application to the assessment of climatic impact on concentrations of sulfur

- dioxide and nitrogen oxides in Hong Kong, *Atmos. Environ.*, 34, 585–594, 2000.
- Cobourn, W. G., Dolcine, L., French, M., and Hubbard, M. C.: A comparison of nonlinear regression and neural network models for ground-level ozone forecasting, *J. Air Waste Manage. Assoc.*, 50, 1999–2009, 2000.
- Cobourn, W. G.: Accuracy and reliability of an automated air quality forecast system for ozone in seven Kentucky metropolitan areas, *Atmos. Environ.*, 41, 5863–5875, 2007.
- Comrie, A. C.: An enhanced synoptic climatology of ozone using a sequencing technique, *Phys. Geogr.*, 13, 53–65, 1992.
- Comrie, A. C. and Yarnal, B.: Relationships between Synoptic-Scale Atmospheric Circulation and Ozone Concentrations in Metropolitan Pittsburgh, Pennsylvania, *Atmos. Environ.*, 26, 301–312, 1992.
- Comrie, A. C.: Comparing neural networks and regression models for ozone forecasting, *J. Air Waste Manage. Assoc.*, 47, 653–663, 1997.
- D'Andrea, F., Tibaldi, S., Blackburn, M., Boer, G., Deque, M., Dix, M. R., Dugas, B., Ferranti, L., Iwasaki, T., Kitoh, A., Pope, V., Randall, D., Roeckner, E., Straus, D., Stern, W., Van den Dool, H., and Williamson, D.: Northern Hemisphere atmospheric blocking as simulated by 15 atmospheric general circulation models in the period 1979–1988, *Clim. Dynam.*, 14, 385–407, 1998.
- Davies, T. D., Kelly, P. M., Low, P. S., and Pierce, C. E.: Surface Ozone Concentrations in Europe – Links with the Regional-Scale Atmospheric Circulation, *J. Geophys. Res.-Atmos.*, 97, 9819–9832, 1992a.
- Davies, T. D., Farmer, G., Kelly, P. M., Glover, G. M., Apsimon, H. M., and Barthelmie, R. J.: Surface Pressure Pattern Indicators of Mean Monthly Pollutant Concentrations in Southern Scandinavian Precipitation - a Test Using Case-Studies of Months with High and Low Concentrations of Nonmarine Sulfate and Nitrate, *Atmos. Environ.*, 26, 261–278, 1992b.
- Davis, J. M. and Speckman, P.: A model for predicting maximum and 8 h average ozone in Houston, *Atmos. Environ.*, 33, 2487–2500, 1999.
- de Arellano, Jordi Vila-Guerau, Duynkerke, P. G., Jonker, P. J., and Builtjes, P. J. H.: An observational study on the effects of time and space averaging in photochemical models, *Atmos. Environ.*, 27, 353–362, 1993.
- Delcloo, A. W. and De Backer, H.: Modelling planetary boundary layer ozone, using meteorological parameters at Uccle and Payenne, *Atmos. Environ.*, 39, 5067–5077, 2005.
- Delcloo, A. W. and De Backer, H.: Five day 3D back trajectory clusters and trends analysis of the Uccle ozone sounding time series in the lower troposphere (1969–2001), *Atmos. Environ.*, 42, 4419–4432, 2008.
- Demuzere, M., Werner, M., Van Lipzig, N. P. M., and Roeckner, E.: An analysis of present and future ECHAM5 pressure fields using a classification of circulation patterns, *Int. J. Climatol.*, 28(1), 1–15, doi:10.1002/joc.1821, 2008.
- European Union: Council Directive 1999/39/EC of 22 April 1999 regulating to limit values for sulphur dioxide, nitrogen dioxide and oxides of nitrogen, particulate matter and lead in ambient air, *Official Journal of the European Communities*, L163, 0041–0060, 1999.
- European Union: Directive 2008/50/EC of the European Parliament and of the council of 21 May 2008 on ambient air quality and cleaner air for Europe. *Official Journal of the European Union L 152/1*, 2008.
- Flemming, J., Stern, R., and Yamartino, R. J.: A new air quality regime classification scheme for O<sub>3</sub>, NO<sub>2</sub>, SO<sub>2</sub> and PM<sub>10</sub> observations sites, *Atmos. Environ.*, 39, 6121–6129, 2005.
- Gardner, M. W. and Dorling, S. R.: Artificial neural networks (the multilayer perceptron) – A review of applications in the atmospheric sciences, *Atmos. Environ.*, 32, 2627–2636, 1998.
- Gardner, M. W. and Dorling, S. R.: Neural network modelling and prediction of hourly NOx and NO<sub>2</sub> concentrations in urban air in London, *Atmos. Environ.*, 33, 709–719, 1999.
- Gardner, M. W. and Dorling, S. R.: Meteorologically adjusted trends in UK daily maximum surface ozone concentrations, *Atmos. Environ.*, 34, 171–176, 2000.
- Giorgi, F. and Meleux, F.: Modelling the regional effects of climate change on air quality, *Comp. Rend. Geosci.*, 339, 721–733, 2007.
- Goyal, P., Chan, A. T., and Jaiswal, N.: Statistical models for the prediction of respirable suspended particulate matter in urban cities, *Atmos. Environ.*, 40, 2068–2077, 2006.
- Graedel, T. E. and Crutzen, P. J.: *Atmospheric Change: An Earth System Prospective*, Freeman, New York, USA, 1993.
- Grivas, G. and Chaloulakou, A.: Artificial neural network models for prediction of PM<sub>10</sub> hourly concentrations, in the Greater Area of Athens, Greece, *Atmos. Environ.*, 40, 1216–1229, 2006.
- Guicherit, R. and Van Dop, H.: Photochemical production of ozone in western Europe (1971–1975) and its relation to meteorology, *Atmos. Environ.*, 11, 145–155, 1977.
- Harrison, R. M., Deacon, A. R., Jones, M. R., and Appleby, R. S.: Sources and processes affecting concentrations of PM<sub>10</sub> and PM<sub>2.5</sub> particulate matter in Birmingham (UK), *Atmos. Environ.*, 31, 4103–4117, 1997.
- Hess, P. and Brezowsky, H.: *Katalog der Großwetterlagen Europas*. Ber. Dt. Wetterd. in der US-Zone 33, Bad Kissingen, Germany, 1952.
- Hooyberghs, J., Mensink, C., Dumont, G., Fierens, F., and Brasseur, O.: A neural network forecast for daily average PM<sub>10</sub> concentrations in Belgium, *Atmos. Environ.*, 39, 3279–3289, 2005.
- Hubbard, M. C. and Cobourn, W. G.: Development of a regression model to forecast ground-level ozone concentration in Louisville, KY, *Atmos. Environ.*, 32, 2637–2647, 1998.
- Huth, R., Beck, C., Philipp, A., Demuzere, M., Ustrnul, Z., Cahynová, M., Kysely, K., and Tveito, O. E.: Classifications of atmospheric circulation patterns: recent advances and applications, *Annals of the New York Academy of sciences*, 1146, 105–152, 2008.
- Intergovernmental Panel on Climate Change (IPCC): the Physical Science Basis, Contribution of Working Group I to the Fourth Assessment Report of the IPCC 2007, available online at: <http://www.ipcc.ch>, 2007.
- Jacobson, M. Z.: On the causal link between carbon dioxide and air pollution mortality, *Geophys. Res. Lett.*, 35(3), 1–5, 2008.
- Jenkinson, A. F. and Collison, B. P.: An initial climatology of gales of the North Sea, *Synoptic climatology Branch Memorandum*, 62, 1977.
- Jol, A. and Kielland, G. (Eds.): *Air Pollution in Europe 1997*, European Environment Agency, Copenhagen, Denmark, 1997.
- Jones, P. D., Hulme, M., and Briffa, K. R.: A Comparison of Lamb Circulation Types with an Objective Classification Scheme, *Int.*

- J. Climatol., 13, 655–663, 1993.
- Jones, P. D., Hulme, M., and Briffa, K. R.: A Comparison of Lamb Circulation Types with an Objective Classification Scheme, *Int. J. Climatol.*, 13, 655–663, 1993.
- Kalkstein, L. S. and Corrigan, P.: A Synoptic Climatological Approach For Geographical Analysis: Assessment of Sulfur Dioxide Concentrations, *Ann. Assoc. Am. Geogr.*, 76, 381–395, 1986.
- Kalkstein, L. S., Nichols, M. C., Barthel, C. D., and Greene, J. S.: A new spatial synoptic classification: Application to air-mass analysis, *Int. J. Climatol.*, 16, 983–1004, 1996.
- Kassomenos, P. A., Sindosi, O. A., Lolis, C. J., and Chaloulakou, A.: On the relation between seasonal synoptic circulation types and spatial air quality characteristics in Athens, Greece, *J. Air Waste Manage. Assoc.*, 53, 309–324, 2003.
- Kruskal, H. and Wallis, W. A.: Use of ranks in one-criterion variance analysis, *J. Am. Stat. Assoc.*, 47, 583–621, 1952.
- Kukkonen, J., Partanen, L., Karppinen, A., Ruuskanen, J., Junninen, H., Kolehmainen, M., Niska, H., Dorling, S., Chatterton, T., Foxall, R., and Cawley, G.: Extensive evaluation of neural network models for the prediction of NO<sub>2</sub> and PM<sub>10</sub> concentrations, compared with a deterministic modelling system and measurements in central Helsinki, *Atmos. Environ.*, 37, 4539–4550, 2003.
- Lasry, F., Coll, I., and Buisson, E.: An insight into the formation of severe ozone episodes: modeling the 21/03/01 event in the ESCOMPTE region, *Atmos. Res.*, 74, 191–215, 2005.
- Lu, H. C., Hsieh, J. C., and Chang, T. S.: Prediction of daily maximum ozone concentrations from meteorological conditions using a two-stage neural network, *Atmos. Res.*, 81, 124–139, 2006.
- Medina, S., Plasencia, A., Ballester, F., Mucke, H. G., Schwartz, J.: Aphis: public health impact of PM<sub>10</sub> in 19 European cities, *J. Epidem. Comm. Health*, 58, 831–836, 2004.
- Mondal, R., Sen, G. K., Chatterjee, M., Sen, B. K., and Sen, S.: Ground-level concentration of nitrogen oxides (NO<sub>x</sub>) at some traffic intersection points in Calcutta, *Atmos. Environ.*, 34, 629–633, 2000.
- Norusis, M. J.: SPSS 11.0 guide to data analysis, Upper saddle River, NJ, Prentice Hall, 2002.
- NRC: Human exposure assessment for airborne pollution: advances and opportunities, National Academy Press, Washington DC, USA, 321 pp., 1991.
- Murphy, A. H.: Skill scores based on the mean square error and their relationship to the correlation coefficient, *Mon. Weather Rev.*, 116, 2417–2424, 1988.
- Nunnari, G., Nucifora, A. F. M., and Randieri, C.: The application of neural techniques to the modelling of time-series of atmospheric pollution data, *Ecol. Model.*, 111, 187–205, 1998.
- Oanh, N. T. K., Chutimon, P., Ekbordin, W., and Supat, W.: Meteorological pattern classification and application for forecasting air pollution episode potential in a mountain-valley area, *Atmos. Environ.*, 39, 1211–1225, 2005.
- Papanastasiou, D. K., Melas, D., and Kioutsioukis, I.: Development and assessment of neural network and multiple regression models in order to predict PM<sub>10</sub> levels in a medium-sized mediterranean city, *Water Air Soil Poll.*, 182, 325–334, 2007.
- Perez, P., Trier, A., and Reyes, J.: Prediction of PM<sub>2.5</sub> concentrations several hours in advance using neural networks in Santiago, Chile, *Atmos. Environ.*, 34, 1189–1196, 2000.
- Perez, P.: Prediction of sulfur dioxide concentrations at a site near downtown Santiago, Chile, *Atmos. Environ.*, 35, 4929–4935, 2001.
- Reich, S. L., Gomez, D. R., and Dawidowski, L. E.: Artificial neural network for the identification of unknown air pollution sources, *Atmos. Environ.*, 33, 3045–3052, 1999.
- Reis, S., Simpson, D., Friedrich, R., Jonson, J. E., Unger, S., and Obermeier, A.: Road traffic emissions - predictions of future contributions to regional ozone levels in Europe, *Atmos. Environ.*, 34, 4701–4710, 2000.
- Santer, B. D., Wigley, T. M. L., Boyle, J. S., Gaffen, D. J., Hnilo, J. J., Nychka, D., Parker, D. E., and Taylor, K. E.: Statistical significance of trends and trend differences in layer-average atmospheric temperature time series, *J. Geophys. Res.-Atmos.*, 105, 7337–7356, 2000.
- Satsangi, G. S., Lakhani, A., Kulshrestha, P. R., and Taneja, A.: Seasonal and diurnal variation of surface ozone and a preliminary analysis of exceedance of its critical levels at a semi-arid site in India, *J. Atmos. Chem.*, 47, 271–286, 2004.
- Schaap, M., Apituley, A., Timmermans, R. M. A., Koelemeijer, R. B. A. and de Leeuw, G.: Exploring the relation between aerosol optical depth and PM<sub>2.5</sub> at Cabauw, the Netherlands, *Atmos. Chem. Phys.*, 9, 909–925, 2009, <http://www.atmos-chem-phys.net/9/909/2009/>.
- Schlink, U., Herbarth, O., Richter, M., Dorling, S., Nunnari, G., Cawley, G., and Pelikan, E.: Statistical models to assess the health effects and to forecast ground-level ozone, *Environ. Model. Softw.*, 21, 547–558, 2006.
- Seinfeld, J. H. and Pandis, S. N.: Atmospheric chemistry and physics from air pollution to climate change, New York, John Wiley & Sons, Inc, 1113 pp., 1998.
- Semazzi, F.: Air quality research: perspective from climate change modelling research, *Environ. Int.*, 29, 253–261, 2003.
- Sillman, S.: The relation between ozone, NO<sub>x</sub> and hydrocarbons in urban and polluted rural environments, *Atmos. Environ.*, 33, 1821–1845, 1999.
- Sillman, S. and He, D. Y.: Some theoretical results concerning O<sub>3</sub>-NO<sub>x</sub>-VOC chemistry and NO<sub>x</sub>-VOC indicators, *J. Geophys. Res.-Atmos.*, 107, 26–41, 2002.
- Smith, R. L., Davis, J. M., Sacks, J., Speckman, P., and Styer, P.: Regression models for air pollution and daily mortality: analysis of data from Birmingham, Alabama, *Environmetrics*, 11, 719–743, 2000.
- Slini, T., Kaprara, A., Karatzas, K., and Moussiopoulos, N.: PM<sub>10</sub> forecasting for Thessaloniki, Greece, *Environ. Model. Softw.*, 21, 559–565, 2006.
- Stadlober, E., Hormann, S., and Pfeiler, B.: Quality and performance of a PM<sub>10</sub> daily forecasting model, *Atmos. Environ.*, 42, 1098–1109, 2008.
- Styer, P., Mcmillan, N., Gao, F., Davis, J., and Sacks, J.: Effect of Outdoor Airborne Particulate Matter on Daily Death Counts, *Environ. Health Perspect.*, 103, 490–497, 1995.
- Sousa, S. I. V., Martins, F. G., Alvim-Ferraz, M. C. M., and Pereira, M. C.: Multiple linear regression and artificial neural networks based on principal components to predict ozone concentrations, *Environmental Modelling & Software* 22, 97–103, 2007.
- Trigo, R. M. and DaCamara, C. C.: Circulation weather types and their influence on the precipitation regime in Portugal, *Int. J. Climatol.*, 20, 1559–1581, 2000.
- Trigo, R. M., Trigo, I. F., DaCamara, C. C., and Osborn, T. J.: Cli-

- mate impact of the European winter blocking episodes from the NCEP/NCAR Reanalyses, *Clim. Dynam.*, 23, 17–28, 2004.
- Tulet, P., Crassier, V., and Rosset, R.: Air pollution modelling at a regional scale, *Environ. Model. Softw.*, 15, 693–701, 2000.
- van der Wal, J. T. and Janssen, L. H. J. M.: Analysis of spatial and temporal variations of PM<sub>10</sub> concentrations in the Netherlands using Kalman filtering, *Atmos. Environ.*, 34, 3675–3687, 2000.
- Warneck P.: *Chemistry of the Natural Atmosphere*, 2nd ed., International Geophysics Series Vol.71, Academic Press, New York, USA, 1998.
- Wilks, D. S.: *Statistical Methods in the Atmospheric Sciences*, Academic Press, San Diego, CA, USA, 476 pp., 1995.
- Wise, E. K. and Comrie, A. C.: Meteorologically adjusted urban air quality trends in the Southwestern United States, *Atmos. Environ.*, 39, 2969–2980, 2005.
- WHO: *Air quality guidelines for Europe*, 2nd ed. Copenhagen, World Health Organization Regional Office for Europe, 2000 (WHO Regional Publications, European Series No. 91), 2000.
- WHO: *World Health Organisation air quality guidelines for particulate matter, ozone, nitrogen dioxide and sulfur dioxide, global update 2005, Summary of risk assessment*, World Health Organization Regional Office for Europe, 2005.
- Yarnal, B.: *Synoptic climatology in environmental analysis*, London, Belhaven Press, 195 pp., 1993.
- Ziomas, I. C., Melas, D., Zerefos, C. S., Bais, A. F., and Paliatoss, A. G.: Forecasting peak pollutant levels from meteorological variables, *Atmos. Environ.*, 29, 3703–3711, 1995.